

RESEARCH ARTICLE | *Translational Physiology*

Chip-based sensing for release of unprocessed cell surface proteins in vitro and in serum and its (patho)physiological relevance

 **Günter A. Müller,¹ Andreas W. Herling,² Kerstin Stemmer,¹ Andreas Lechner,^{3,4} and Matthias H. Tschöp^{1,5,6}**

¹Institute for Diabetes and Obesity, Helmholtz Diabetes Center at Helmholtz Zentrum München, Neuherberg, Germany;

²Sanofi Deutschland GmbH, Diabetes Research Division, Frankfurt am Main, Germany; ³Diabetes Research Group, Medizinische Klinik IV, Medical Center, Ludwig-Maximilians-Universität München (Klinikum der Universität München), München, Germany;

⁴Clinical Cooperation Group Type 2 Diabetes, Helmholtz Zentrum München,

Oberschleissheim/Neuherberg, Germany; ⁵Division of Metabolic Diseases, Department of Medicine, Technische Universität München, München, Germany; and

⁶German Center for Diabetes Research, Oberschleissheim/Neuherberg, Germany

Submitted 27 February 2019; accepted in final form 29 April 2019

Müller GA, Herling AW, Stemmer K, Lechner A, Tschöp MH.

Chip-based sensing for release of unprocessed cell surface proteins in vitro and in serum and its (patho)physiological relevance. *Am J Physiol Endocrinol Metab* 317: E212–E233, 2019. First published April 30, 2019; doi:10.1152/ajpendo.00079.2019.—To study the possibility that certain components of eukaryotic plasma membranes are released under certain (patho)physiological conditions, a chip-based sensor was developed for the detection of cell surface proteins, which are anchored at the outer leaflet of eukaryotic plasma membranes by a covalently attached glycolipid, exclusively, and might be prone to spontaneous or regulated release on the basis of their amphiphilic character. For this, unprocessed, full-length glycosylphosphatidylinositol-anchored proteins (GPI-AP), together with associated phospholipids, were specifically captured and detected by a chip- and microfluidic channel-based sensor, leading to changes in phase and amplitude of surface acoustic waves (SAW) propagating over the chip surface. Unprocessed GPI-AP in complex with lipids were found to be released from rat adipocyte plasma membranes immobilized on the chip, which was dependent on the flow rate and composition of the buffer stream. The complexes were identified in the incubation medium of primary rat adipocytes, in correlation to the cell size, and in rat as well as human serum. With rats, the measured changes in SAW phase shift, reflecting specific mass/size or amount of the unprocessed GPI-AP in complex with lipids, and SAW amplitude, reflecting their viscoelasticity, enabled the differentiation between the lean and obese (high-fat diet) state, and the normal (Wistar) and hyperinsulinemic (Zucker fatty) as well as hyperinsulinemic hyperglycemic (Zucker diabetic fatty) state. Thus chip-based sensing for complexes of unprocessed GPI-AP and lipids reveals the inherently labile anchorage of GPI-AP at plasma membranes and their susceptibility for release in response to (intrinsic/extrinsic) cues of metabolic relevance and may, therefore, be useful for monitoring of (pre-)diabetic disease states.

adipocytes; biosensor; diabetes; glycolipid-anchored cell surface proteins; metabolic stress; obesity

INTRODUCTION

Glycosylphosphatidylinositol-anchored proteins (GPI-AP), which represent ~1% of all proteins in eukaryotes, are cell surface proteins and constituted by a variably large hydrophilic protein moiety and a highly conserved hydrophobic glycolipid (GPI), which serves as anchor at the extracellular leaflet of plasma membranes (11, 12, 49) (Fig. 1A). On the basis of their amphiphilic overall nature and the exclusive membrane anchorage via the GPI moiety, which is putatively less stringent than that of typical transmembrane proteins, GPI-AP may be regarded as candidates for spontaneous or regulated release from plasma membranes upon exposure to endogenous (e.g., surface tension of hypertrophic fat cells) or exogenous (e.g., high serum concentration of fatty acids and albumin) cues, which are typically prevalent during metabolic stress, such as type 2 diabetes (T2D) and obesity.

In contrast to the well-documented shedding of processed soluble GPI-AP (as a result of lipolytic cleavage of the GPI anchor or proteolytic cleavage of the protein moiety) (39, 49), the release of the unprocessed amphiphilic GPI-AP carrying the full-length GPI moiety may necessitate embedding of its long-chain saturated fatty acyl chains into macromolecular structures. Those would prevent access of the aqueous environment and may be composed of mixed phospholipid micelles (Fig. 1B), vesicles, lipoprotein- or surfactant-like particles, or binding proteins for hydrophobic ligands. The rate of release of those structures from plasma membranes of relevant cells may depend on their intrinsic morphological and biophysical characteristics, as well as on extrinsic factors, such as mechanical forces (leading to stretching or compression of the cell shape) or plasma constituents, such as reactive oxygen species, lipids or free fatty acids.

This rationale for the approach presented with the aim to identify and characterize unprocessed GPI-AP in complex with additional constituents in extracellular fluids is supported by the following previous experimental findings. 1) Some GPI-AP, among them CD73 and Gce1, have been reported to be released from primary and cultured adipocytes with their complete GPI anchor still attached in response to high extracellular concentrations of palmitate, H₂O₂, and the anti-diabetic drug, glimepiride (40, 50, 77). 2) Phospholipids have been detected

Address for reprint requests and other correspondence: G. A. Müller, Institute for Diabetes and Obesity (IDO), Helmholtz Diabetes Center (HDC) at Helmholtz Zentrum, Ingolstädter Landstraße 1, D-85764 Oberschleissheim/Neuherberg, Germany (e-mail: guenter.mueller@helmholtz-muenchen.de).

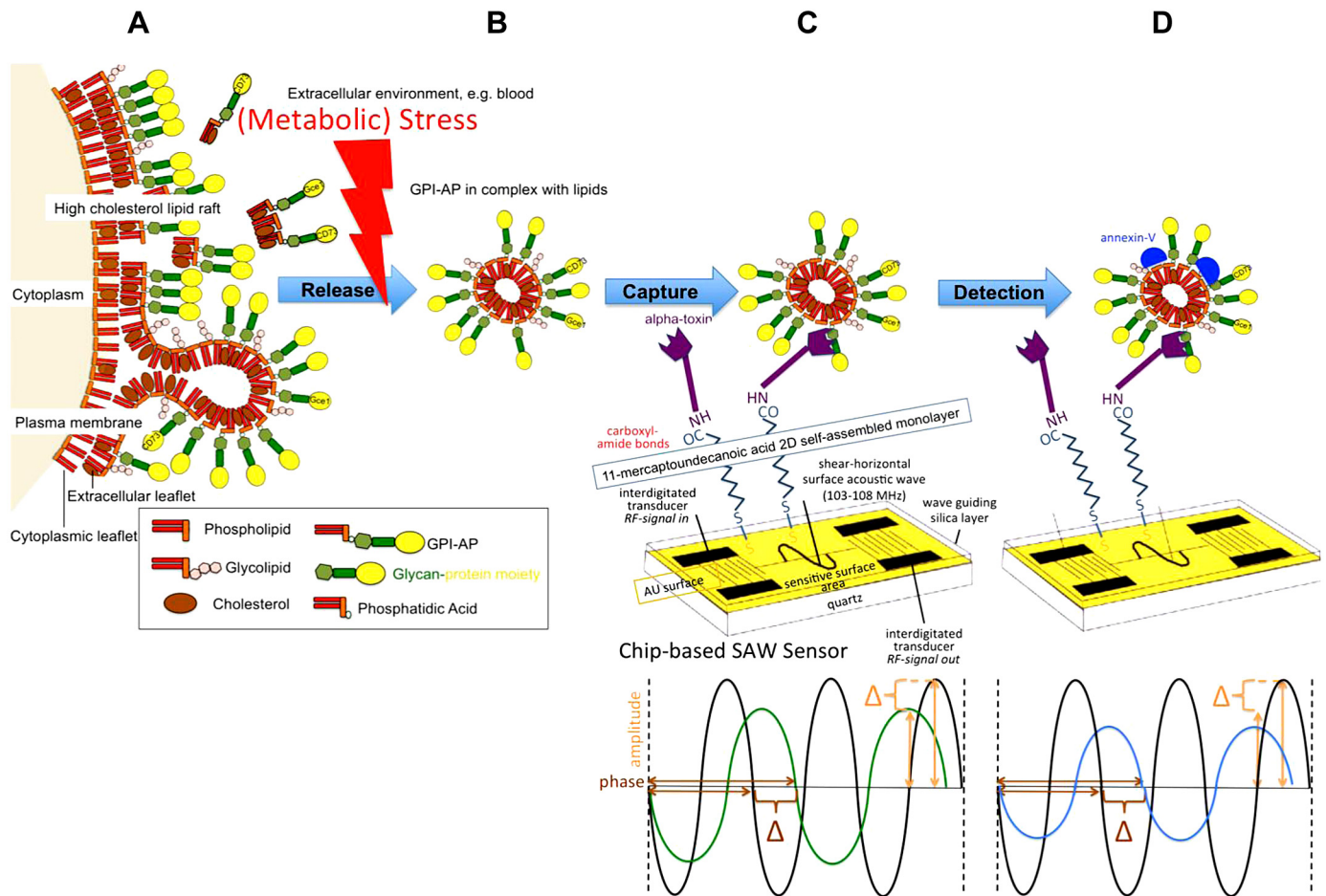


Fig. 1. Principle of the chip-based sensing of unprocessed glycosylphosphatidylinositol-anchored proteins (GPI-AP) in complex with lipids. **A:** GPI-AP enriched at high-cholesterol-containing lipid rafts of plasma membranes are released from the extracellular leaflet into the environment (e.g., blood) in response to (metabolic) stress without the involvement of lipolytic or proteolytic processing. **B:** unprocessed GPI-AP are in complex with cholesterol and phospholipids and may form micelle-like structures. **C:** specific capture of the GPI-AP by the chip-based surface acoustic wave sensor is accomplished by binding to α -toxin. Covalent coupling of α -toxin to the chip gold surface is performed using the conventional 1-ethyl-3-(3-dimethylaminopropyl)carbodiimide/sulfo-*N*-hydroxysulfosuccinimide-based protocol and is monitored by measuring the phase shift in the course of the reaction (see Supplemental Fig. S1; <https://doi.org/10.6084/m9.figshare.7994312.v1>). Signals generated by the sensor and recorded in real time reflect the loading of mass onto the chip surface and, in addition, depend on the (bio)physical properties of the contacting sample fluid, predominantly its viscoelasticity. Capture of the unprocessed GPI-AP leads to rightward shifts in phase and/or reductions in amplitude of the shear-horizontal surface acoustic wave propagating along the chip surface (green curve) vs. blank chip (black curve). **D:** phospholipids in complex with the unprocessed GPI-AP become detected in the course of sequential binding “in sandwich” of the Ca^{2+} -dependent phospholipid-sequestering protein annexin V, which leads to further rightward shift in phase and reduction in amplitude (blue curve) vs. blank chip (black curve), as indicated by brown and orange triangles/arrows, respectively.

in plasma by untargeted lipidomics and shown to correlate with early signs of neurodegeneration during presymptomatic Alzheimer disease (8, 75). 3) GPI-AP have been found to be transferred from donor to acceptor cells in vitro and in vivo under maintenance of their original function (1, 54, 55). This putative transmission of biological material or information within or between tissues holds true for GPI-AP with the unprocessed GPI anchor attached, but not for their lipolytically or proteolytically processed counterparts (29, 38, 63). 4) The GPI-AP, CD73, has been measured in plasma, and its concentration demonstrated to correlate with insulin sensitivity in diabetic mice and human subjects (34, 52). 5) Phospholipids in complex with certain membrane proteins have been identified in the incubation medium of cultured vascular endothelial cells and in plasma of mice exposed to oxidative and shearing stress, as well as a high-fat diet (35, 78). 6) GPI-AP harboring the glycan core of the GPI anchor have been measured at increased

levels in the plasma of patients suffering from glioblastoma brain tumors, lower grade colon adenocarcinomas, and ovarian cancer, which presumably causes the generation of oxygen radicals and metabolic stress compared with healthy subjects (10). 7) GPI-AP have been identified as constituents of vesicle- and lipoprotein-like structures in human plasma (48, 56, 70). 8) The identification in serum of GPI-AP protein moieties, separated from the GPI anchor by lipolytic or proteolytic cleavage (39), apparently is not very informative, since proteomic analysis of serum should already have recognized those fragments and differences in their level in correlation to (stress-related) diseases.

Since the amount of unprocessed GPI-AP in extracellular fluids is likely to be rather low, the typical commonly used techniques for studying the secretome, such as 2D-PAGE, mass spectrometry, immunoblotting, and ELISA, have to be combined with time-consuming and tedious procedures for

prior fractionation and enrichment of low-abundance proteins. However, those may not be successful for GPI-AP in association with amphiphilic constituents, such as phospholipids, since centrifugation, flotation, and SDS-PAGE in the course of sample preparation and solubilization may lead to loss or disruption of the complexes and be incompatible with the required analytical sensitivity and resolution, as well as with throughput measurements. To avoid isolation of the presumably labile complexes between GPI-AP and other constituents and to enable their specific and sensitive detection and biophysical characterization in extracellular fluids, such as serum, a homogenous assay design based on a chip- and microfluidic channel-based sensing system was developed. It relies on the propagation of horizontal surface acoustic waves (SAW) along the chip gold surface, which is affected by interaction of any molecule with the surface (2, 14, 17, 27, 58). The resulting alterations in frequency and amplitude of the SAW reflect changes in mass loading and viscoelasticity and are thus correlated to the presence of the analyte and its biophysical characteristics (9, 13, 18, 72). The major advantages of SAW compared with optical sensors seem to be their compatibility with turbid and complex matrices, in combination with high sensitivity toward alterations in the amount, mass, and viscoelasticity of the analyte (2, 19, 32, 72).

For specific capturing of unprocessed GPI-AP, the chip surface was coated with α -toxin, which interacts with the glycan core of GPI-AP (16). The presence of phospholipids in complex with the GPI-AP was then monitored by binding of annexin V. Using this setting of chip-based sensing, unprocessed GPI-AP in complex with phospholipids were detected in incubation media of isolated adipocyte plasma membranes and adipocytes, as well as in rat and human serum. The release was found to depend on the milieu surrounding the plasma membranes and the genotype/phenotype of the donor organism. The findings hint at a moderately stable cell surface anchorage of GPI-AP, in particular on exposure to metabolic stress, which may be useful for monitoring of obesity and T2D.

MATERIALS AND METHODS

Preparation of α -Toxin

α -Toxin was purified from the culture supernatant of *Clostridium septicum* (strain KZ1003) after an 18-h culture in brain-heart infusion broth (Difco). After precipitation by 60% saturated ammonium sulfate and centrifugation, the pellet was dissolved in 10 mM sodium phosphate (pH 7.0) and then subjected to cation exchange chromatography on SP-Toyopearl 650M (24). After elution, the corresponding fraction was again precipitated by 60% saturated ammonium sulfate and centrifuged. SDS-PAGE and Coomassie staining of the pellet materials resulted in a single protein band at a position corresponding to a molecular mass of 48 kDa. α -Toxin was suspended in 100 mM 2-[N-morpholino]ethanesulfonic acid (MES)/KOH (pH 6.5) at 1 mg/ml.

Coupling of α -Toxin to Microspheres

5.0×10^6 of the uncoupled magnetic carboxylated microspheres (MagPlex-C, Lumines) in a microcentrifuge tube were resuspended according to the instructions of the product information sheet, placed into a magnetic separator, and then subjected to separation for 30–60 s. After removal of the supernatant and subsequently of the tube from the separator, the microspheres were resuspended in 100 μ l of double-distilled H₂O twice daily by vortexing and sonication for

~20 s. Thereafter the tube was again placed into the magnetic separator, and separation was allowed to occur for 30–60 s. After removal of the supernatant and subsequently of the tube from the separator, the washed microspheres were resuspended in 80 μ l of 100 mM sodium phosphate (pH 6.2) by vortexing and sonication for ~20 s. After addition of 10 μ l of 50 mg/ml sulfo-N-hydroxysulfosuccinimide (NHS) (diluted in double-distilled H₂O) to the microspheres and gentle mixing by vortexing, they were supplemented with 10 μ l of 50 mg/ml 1-ethyl-3-(3-dimethylaminopropyl)carbodiimide (EDC) (diluted in double-distilled H₂O). The mixture was incubated (20 min, 22°C) under gentle mixing by vortexing at 5-min intervals. Subsequently, the tube was placed into the magnetic separator, and separation was allowed to occur for 30–60 s. The supernatant was removed, and then the tube was removed from the separator. The activated microspheres were resuspended in 250 μ l of 50 mM MES/KOH (pH 5.0) by vortexing and sonication for ~20 s. The washing step with magnetic separation and resuspension in 100 mM MES/KOH (pH 6.5) was repeated three times. After the last separation, the microspheres were suspended in 100 μ l of 100 mM MES/KOH (pH 6.5) by vortexing and sonication for ~20 s. α -Toxin (200 μ g) was added to the activated and washed microspheres, and the total reaction volume was adjusted to 500 μ l of 100 mM MES/KOH (pH 6.5). After vortexing, the mixture was incubated (2 h, 22°C) under head-over rotation. Subsequently, the tube was placed into the magnetic separator, and separation was allowed to occur for 30–60 s. The supernatant was removed, and then the tube from the separator was removed. The coupled microspheres were resuspended in 500 μ l of PBS/TBN (PBS, pH 7.4, 0.1% BSA, 0.02% Tween 20, and 0.05% azide) by vortexing and sonication for 20 s. After incubation (30 min, 22°C) under head-over rotation, the microspheres were subjected to magnetic separation for 30–60 s. The supernatant was removed, and then the tube from the separator was removed. The microspheres were resuspended in 1 ml of PBS/TBN by vortexing and sonication for 20 s. The washing step with magnetic separation and resuspension was repeated three times with 1 ml each of PBS. After the last separation, coupled and washed microspheres were suspended in 500 μ l of PBS/TBN by vortexing and sonication for ~20 s and then stored at 4°C in the dark.

Depletion of Samples from GPI-Harboring Entities

Medium samples. Ten milliliters of incubation medium were added to 500 μ l of PBS containing the microspheres coupled to α -toxin in a 15-ml vial. After vortexing, the mixtures were incubated (30 min, 22°C) under head-over rotation. Subsequently, the tubes were placed into the magnetic separator, and separation was allowed to occur for 30–60 s. The supernatants were removed, and then the tube from the separator was removed. The coupled microspheres were resuspended in 500 μ l of PBS/TBN by vortexing and sonication for 20 s. After incubation (30 min, 22°C) under head-over rotation, the microspheres were subjected to magnetic separation for 30–60 s. The supernatant was removed, and then the tube from the separator was removed. The microspheres were resuspended in 1 ml of PBS/TBN by vortexing and sonication for 20 s. The washing step with magnetic separation and resuspension was repeated three times with 1 ml of PBS each.

Serum samples. Microspheres (1×10^5) coupled to α -toxin and resuspended in 10 μ l of PBS/TBN were added to 90 μ l serum and after vortexing and sonication for 20 s incubated (30 min, 22°C) under head-over rotation. The microspheres were subjected to magnetic separation for 30–60 s. The supernatant was transferred to a new tube, and then the tube was removed from the separator. The microspheres were resuspended in 100 μ l of PBS/TBN by vortexing and sonication for 20 s. After the magnetic separation, the supernatant was removed and combined with the initial supernatant.

Depletion of Samples from Gce1 and CD73

cAMP-agarose and 5'-AMP-agarose [(c)AMP-agarose] or agarose alone were suspended in PBS/TBN at 50 mg/ml. Ten microliters were

added to 90 μl of serum and then incubated (30 min, 22°C) under head-over rotation. Subsequently, the suspensions were subjected to centrifugation (300 g, 5 min, 22°C). The supernatants were transferred to new tubes. The beads in the pellets were resuspended in 100 μl of PBS/TBN by gentle vortexing and then recentrifuged. The supernatants were removed and combined with the initial supernatants.

Coupling of α -Toxin to the Chip Surface

Coupling reactions were performed as described previously (25, 27, 28, 30) with the following modifications. For the generation of chips that capture GPI-AP, α -toxin (in 20 mM Tris-HCl, pH 7.5, 150 mM NaCl, and 10% glycerol) diluted in immobilization buffer (10 mM sodium acetate, pH 5.5) was coupled to the channels of activated long-chain 3D carboxymethyl dextran chips (SAW Instruments, Bonn, Germany) in a SamX instrument (SAW Instruments). For this, the surface of microfluidic channels of sensor chips was primed by three injections of 150 μl each of immobilization buffer at a flow rate of 45 $\mu\text{l}/\text{min}$. Then the chip surface was activated by a 150- μl injection of 0.2 M EDC and 0.05 M sulfo-NHS (mixed from 2 \times stock solutions right before injection) at a flow rate of 45 $\mu\text{l}/\text{min}$. After a waiting period of 1 min, the coat protein (e.g., α -toxin) was coupled by injection of 200- μl portions at a flow rate of 60 $\mu\text{l}/\text{min}$ and subsequent waiting for 2 min. After additional washing with three 150- μl portions of running buffer PBST [PBS containing 0.005% Tween 20 (vol/vol)] at a flow rate of 30 $\mu\text{l}/\text{min}$ and waiting for 5 min, the residual activated groups on the chip surface were capped by injecting 150 μl of 1 M ethanolamine (pH 8.5) at a flow rate of 45 $\mu\text{l}/\text{min}$. For the generation of a “blank” channel lacking coat protein, one channel was activated and blocked with injection of buffer instead of a coat protein. Measurements were performed at 22°C. The flow rates are given in Fig. 2, 3, 4, A and B, 5A, 8, and 9 legends or can be derived from the figures, considering the start and termination points of the solution flow for sample injections or washing cycles, as indicated with green and black arrows, respectively. Chips were regenerated by successive injections of 60 μl of 10 mM glycine (pH 3.5) and 30 μl of 4 M urea, with waiting for 5 min after each injection, and final injection of 300 μl of regeneration buffer (PBS, pH 7.4, 1 M NaCl, 0.03% Tween and 0.5% glycerol) and 300 μl of PBST and were used up to six times without significant loss of capture (through α -toxin) capacity.

SAW Measurement, Instrumentation, and Evaluation

The Seismos NT.X Instrument for SAW chip-based sensor (NanoTemper Technologies, Munich, Germany), formerly SamX (SAW Biosensor, Bonn, Germany) integrates a high-frequency unit, control and reader units, and all fluid handling components required for a systematic buffer and analyte solution handling (S-sens K5). This enables fluidic and electrical contacting of the chip with four independent flow-through microfluidic channels at a stable temperature of 22°C (temperature change = 0.05°C by means of four Peltier elements). Mass loading and loss of elasticity (gain of viscosity) resulting from biomolecular interaction processes on the chip surface will result in phase shift and amplitude reduction, respectively, of the SAW generated by the inverse piezoelectric effect. The instrument was run, and the signals generated were recorded in real-time using a double-frequency measurement mode, as described previously (13, 18, 32, 37, 51, 72) with the following modifications. Measurements were performed with a continuous buffer stream at the flow rates and temperatures indicated. For each chip, the phase shift and amplitude generated by the α -toxin-coated channels were corrected for unspecific non-GPI-mediated interactions by subtraction of the values of the “blank” channel. In addition, in case of medium or serum samples, the values of the sample channels were corrected for a “medium” or “albumin” channel, respectively, which reflects

the unspecific and noncovalent adsorption of medium components or BSA/rabbit serum albumin (RSA) to α -toxin and is generated by injection of incubation medium or 1% BSA/RSA in PBS, respectively, and further processing identical to the sample channels. To avoid the generation of air bubbles (by spontaneous degassing, EDC/NHS reaction, pipetting, or others), the buffers were degassed by applying vacuum (200 mbar for 30 min), and eventual air bubbles were removed immediately before injection (by gently tapping the vial). To avoid blockage of tubing, sterile-filtered buffers (0.2- μm sterile filters) and degassed double-distilled H₂O were used only and visually inspected for lack of particles or other contaminants. To avoid blockages in the system (autosampler, needle, fluidic cell, tubing), it was cleaned after each experiment and on a regular basis weekly and monthly, according to the instructions of the manufacturer.

Statistics

Original data were analyzed and fitted using the FitMaster Origin-based software (Origin) on subtraction of the corresponding values obtained with a blank and/or control channel, as indicated. Statistical significance was determined with unpaired two-tailed *t*-test using GraphPad Prism 6 (version 6.0.2, GraphPad Software) software. (Supplemental material is available at <https://doi.org/10.6084/m9.figshare.7994312.v1>.)

RESULTS

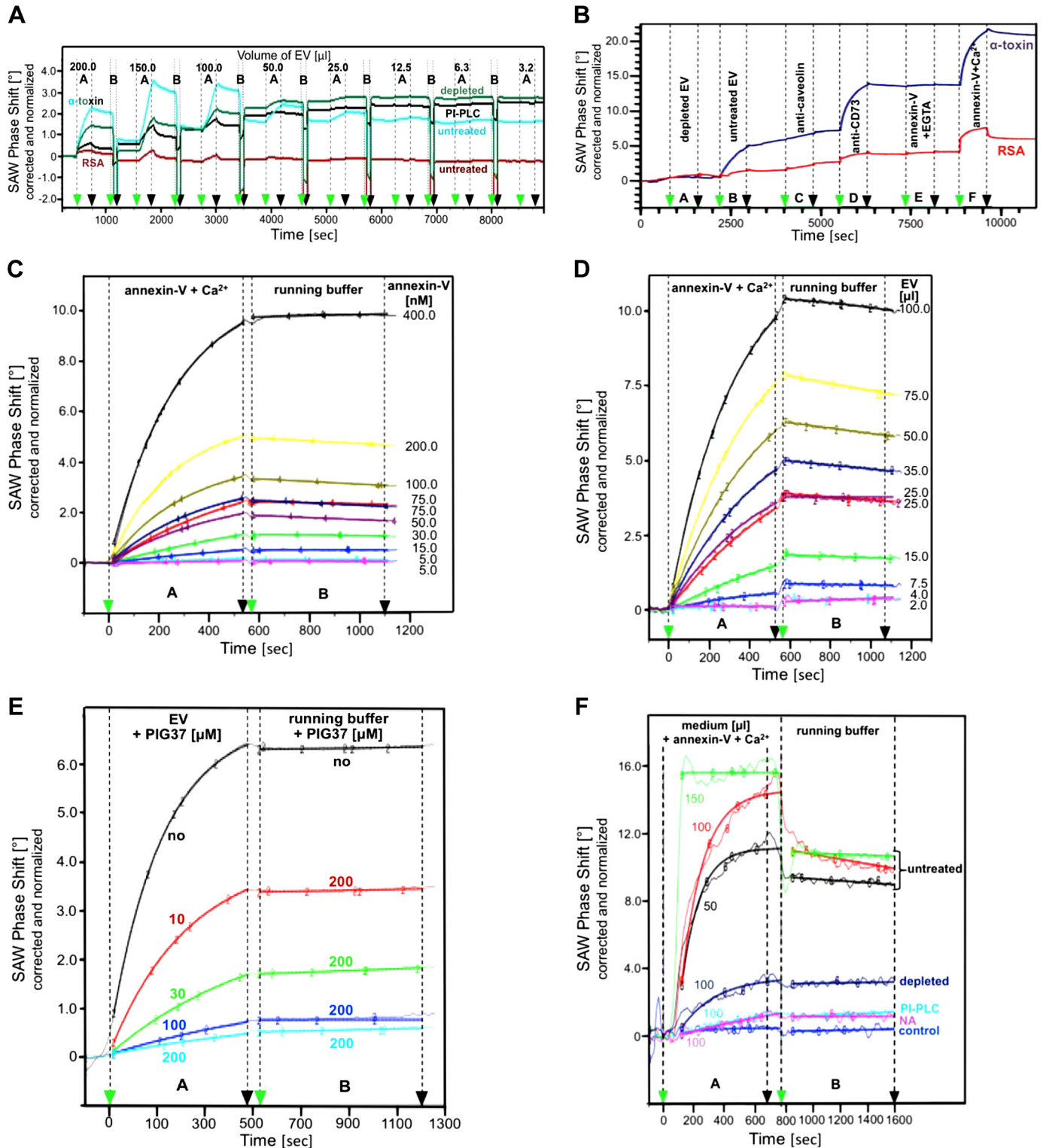
Implementation and Validation of the Sensing Method

The putative release of unprocessed GPI-AP, i.e., with uncleaved full-length GPI anchor, was first studied with adipocytes since their plasma membranes undergo extensive stretching on lipid filling and are in intimate contact with serum albumin and fatty acids. It relies on specific capturing of all GPI-AP, which harbor the conserved GPI glycan core, by the chip gold surface coated with α -toxin, on their injection into the microfluidic channels (Fig. 1C). Coating with α -toxin, which binds to the glycan core of the GPI anchor (16, 24), was performed with conventional coupling chemistry (Supplemental Fig. S1). Any (covalent or secondary) interaction of materials with the chip surface will lead to rightward shifts in phase and/or reductions in amplitude of the horizontal SAW propagating along the chip surface (Fig. 1C). This reflects mass loading and/or increased viscosity, respectively, exerted by the interacting materials (2, 9, 13, 14, 17, 18, 20, 58). Consequently, the coating with α -toxin per se (Supplemental Fig. S1) and the capture of glycan-harboring GPI-AP can be monitored by chip-based sensing (see below).

The sensor was validated using so-called extracellular vesicles (EV) as analytes. EV are membrane vesicles that are released from most cell types (76), in particular on challenge with exogenous stressors (40, 77). A subset of EV released from adipocytes into the incubation medium is known to harbor unprocessed GPI-AP at the outer leaflet of their phospholipid bilayer (7, 46). Injection of EV isolated from rat adipocyte incubation medium into α -toxin-coated, but not into control (i.e., rat serum albumin-coated) chips caused SAW phases shifts, dependent on the volume applied (Fig. 2A). Depletion of the EV from GPI-AP by adsorption to α -toxin-coupled magnetic beads or cleavage of the GPI anchor by bacterial phosphatidylinositol-specific phospholipase C (PI-PLC) before injection (partially) prevented phase shift. The presence of typical GPI-AP, such as CD73, and phospholipids

in (untreated) EV was shown by sequential binding “in sandwich” of anti-CD73 antibodies and the Ca^{2+} -dependent phosphatidylserine-sequestering protein annexin V (in the presence of Ca^{2+} , but not EGTA; Fig. 1D) to the chip (Fig. 2B). The specificity of detection of GPI-AP in complex with phosphatidylserine was confirmed by lack of SAW phase shift using 1)

chips (noncovalently) coated with rat serum albumin; 2) EV depleted from GPI-AP; or 3) antibodies against the non-GPI-anchored membrane protein caveolin, located at the luminal membrane leaflet of the EV (Fig. 2B), as well as by dependence of the SAW phase shift on the annexin V concentration (Fig. 2C) and volume of the EV injected (Fig. 2D) during associa-



tion (*period A*). The specificity of capture of the EV through α -toxin was confirmed by maintenance of the phase shift during washing of the chip surface with running buffer (Fig. 2, *C–F*, *period B*) and its concentration-dependent reduction by the presence of synthetic phosphoinositolglycan (PIG) 37 mimicking the glycan core moiety of GPI-AP (47) during association (Fig. 2*E*, *period A*). Subsequent washing of the captured EV with PIG37 did not cause phase shift decrease, as was true for running buffer alone, compatible with a PIG37-induced delay in association rather than induction of dissociation (Fig. 2*E*). This is presumably due to subtle structural deviation of PIG37 from the authentic GPI glycan core, since PIG41, which resembles it more closely (15), induced the concentration-dependent displacement of captured EV, as well as blockade of recapture of the displaced EV (Supplemental Fig. S2, *periods C* and *F*, respectively).

For a rough calculation of the limit of detection for unprocessed GPI-AP (i.e., having retained glycan core) by chip-based sensing, acetylcholinesterase (AChE) partially purified from detergent extracts of bovine erythrocyte membranes (69) by sequential chromatography on DEAE-cellulose, affinity gel prepared from CNBr-activated Sepharose (5), Sephadex G-75, and finally Sephadex 6B (with a degree of homogeneity of ~50% according to SDS-PAGE and silver staining, as well as the specific activity of 3,200 μmol acetylthiocholine hydrolyzed $\cdot\text{min}^{-1}\cdot\text{mg}$ protein $^{-1}$) was injected into the channels of α -toxin-coated chips. Upon capturing by α -toxin alone (i.e., under omission of monitoring for associated phosphatidylserine by annexin V), a significant increase in phase shift of 0.2° above basal (identical detergent-containing buffer without protein) was observed with 40 μl of 0.30 mg AChE/ml, corresponding to 5 μM (final concentration) and 12 μg AChE in the sample. In the course of removing the diacylglycerol moiety (but not the glycan core) from the GPI anchor of AChE by cleavage with PI-PLC from *Bacillus thuringiensis* (68), the limit of detection decreased moderately but significantly to 0.12 mg AChE/ml, corresponding to 2 μM and 4.8 μg AChE in the sample. Control experiments showed that the apparently higher detection limit for unprocessed compared with lipolytically cleaved AChE is predominantly due to the presence of 0.1% NP-40 in the former samples (for solubilization). However, the sample fluids analyzed in the following (cell and

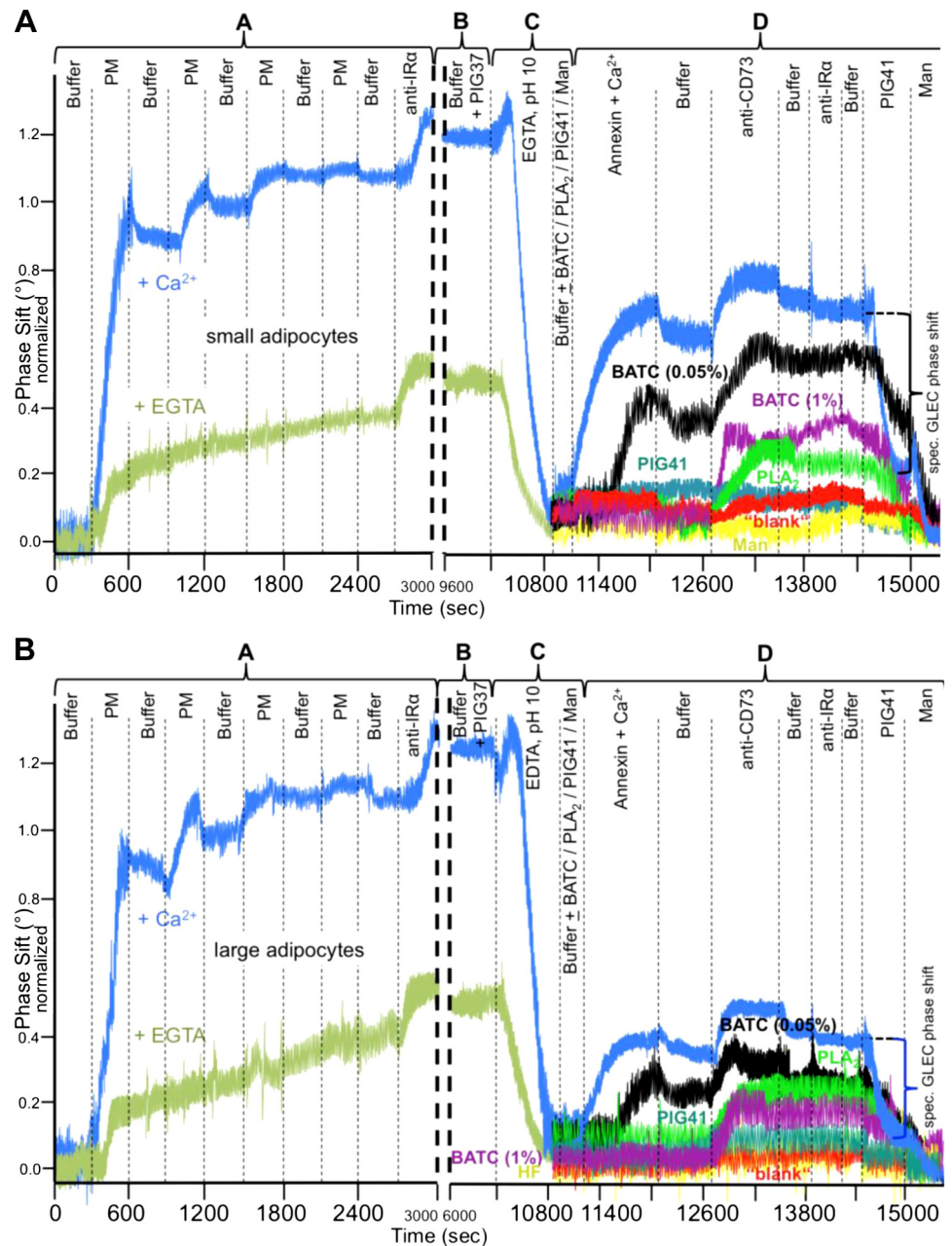
plasma membrane supernatants, serum) did not contain detergent.

Taken together, the sensitivity of the chip-based sensing for solubilized (by either detergent or PI-PLC) GPI-AP harboring the glycan core is about three orders of magnitude lower than that of typical radioimmunoassay or ELISA methods. However, it should be kept in mind that this holds true for the solubilized (monomeric) GPI-AP. GPI-AP in complex with lipids and other proteins may exhibit a considerably lower detection limit for chip-based sensing as a consequence of elevated phase shifts on capturing of analytes with increased (total and specific) mass and size. The ability to detect unprocessed GPI-AP (in the absence of detergent and lipolytic cleavage) in incubation media of adipocytes and plasma membranes and serum samples from rat and humans (see below) is compatible with this hypothesis.

For investigation whether chip-based sensing manages to identify unprocessed GPI-AP, including EV, in crude incubation medium and to differentiate them according to the size of the releasing cell, medium from rat adipocytes of small, medium, and large size, which contains EV at rather low concentration only (40, 44, 77), was used. Adipocyte medium elicited volume-dependent (during capture by α -toxin and detection by annexin V, Fig. 2*F*, *period A*) and stable (during subsequent washing with running buffer, Fig. 2*F*, *period B*) phase shift increases, which were abrogated by depletion of the GPI-AP or cleavage of the GPI anchor by bacterial PI-PLC and nitrous acid deamination. Media from adipocytes of large, medium, and small size (Supplemental Table S1) provoked different association kinetics for the capture of GPI-AP and detection of phospholipids (Supplemental Fig. S3). The injection of 10 and 200 μM PIG37 in the midst of the capture led to maximal differentiation of large vs. medium/small and large/medium vs. small adipocytes, respectively (Supplemental Fig. S4A). Thirty micromolars of PIG37 turned out to enable the simultaneous discrimination of large, medium, and small cells considering phase shift (Supplemental Fig. S4B) and amplitude reduction (Supplemental Fig. S4C). This was maintained during simultaneous detection of phospholipids by annexin V during capture (Supplemental Fig. S4, *B* and *C*). In the absence of PIG37, minor differences between adipocytes of differing size were measured, only (Supplemental Fig. S4C). Final

Fig. 2. Implementation of chip-based sensing of unprocessed glycosylphosphatidylinositol-anchored proteins (GPI-AP). *A*: for capture of rat adipocyte extracellular vesicles (EV), decreasing volumes of EV, which had remained untreated (turquoise and red curves) or had been pretreated with phosphatidylinositol-specific phospholipase C (PI-PLC; black line) or had been depleted for GPI-AP (green curve), were sequentially injected into α -toxin-coated channels (turquoise, black, and green curves) or rabbit serum albumin (RSA; red curve), or into “blank” uncoated channels (see below; *period A*). Phase shift is measured with regeneration after each injection (*period B*) and given (as degrees) on correction for the “blank” channel and normalization (set at 0 for 250 s; see Supplemental Fig. S1A). *B*: for “sandwich” detection of rat adipocyte EV by annexin V and anti-CD73 antibodies, EV, which had been depleted for GPI-AP (*period A*) or left untreated (*period B*), were injected consecutively into α -toxin coated channels (blue curve). For detection of unspecific binding of EV to serum albumin, RSA were injected to yield the “albumin” channel by mere (noncovalent) adsorption (red curve). In addition, uncoated channels were run as “blank” channels. Subsequently, anti-caveolin antibodies (*period C*), anti-CD73 antibodies (*period D*), annexin V containing EGTA (*period E*), and annexin V and Ca^{2+} (*period F*) were injected successively into the channels. *C*: for studying the concentration dependence of the “sandwich” detection of captured EV by annexin V, EV were injected into α -toxin-coated channels or into a “blank” channel. Thereafter, annexin V and Ca^{2+} (*period A*) and then EV buffer (*period B*) were injected. *D*: for studying the volume dependence of capture and detection of adipocyte EV, EV were injected into α -toxin-coated channels or into a “blank” channel. Subsequently, annexin V and Ca^{2+} were injected into all channels (*period A*), followed by injection of EV buffer. *E*: for studying the effect of phosphoinositolglycan 37 (PIG37) on capture of EV, EV in the absence (black curve) or presence of PIG37 (red, green, pink, and blue curves) were injected into α -toxin-coated channels or into a “blank” channel (*period A*). Subsequently, EV buffer containing 200 μM PIG37 or lacking PIG37 was injected (*period B*). *F*: for detection of unprocessed GPI-AP in adipocyte incubation medium, medium obtained by incubation of rat adipocytes of medium size and kept untreated (black, red, and green curves), or depleted for GPI-AP (dark blue curve), or pretreated with PI-PLC (light blue curve) or nitrous acid (NA; pink curve), or medium lacking adipocytes (control; violet curve) were injected into α -toxin-coated channels. Subsequently, annexin V and Ca^{2+} (*period A*) and then buffer were injected (*period B*). For further details, see detailed protocols in data supplements. SAW, surface acoustic wave.

Fig. 3. Implementation of chip-based sensing of plasma membrane (PM)-derived unprocessed glycosylphosphatidylinositol-anchored proteins (GPI-AP) from small or large adipocytes using the “lab-on-the-chip” configuration. For immobilization of PM from small (A) or large (B) adipocytes, three 100- μ l portions (PM) in the presence of EGTA (light green curve) or Ca^{2+} (blue curve) or three portions of running buffer were consecutively injected into α -toxin-coated channels or uncoated “blank” channel (red curve; *period A*). For demonstration of the presence of the insulin receptor α -chain (IR- α), anti-IR- α antibodies were injected at the end of *period A*. For the putative generation of unprocessed GPI-AP from the immobilized PM and their capture by the α -toxin-coated chip, running buffer containing 30 μ M phosphoinositolglycan 37 (PIG37) was injected (*period B*). For release of the PM from the chip surface, glycine (pH 10) containing EGTA was injected, followed by injection of running buffer containing the ingredients indicated. For demonstration of capture of unprocessed GPI-AP, annexin V, and Ca^{2+} , anti-CD73 antibodies, anti-IR- α antibodies, 200 μ M PIG41, and mannose (Man) were injected in that sequential fashion (*period D*). For further details see detailed protocols in data supplements. BATC, 4'-amino-7 β -bezamido-3 α , 12 α , 5 β -taurocholic acid.



injection of PIG41 caused complete abrogation of the medium-induced phase shift (Supplemental Fig. S4B), as well as amplitude reduction (Supplemental Fig. S4C), arguing for the specificity of capture and the possibility of chip reuse after total dissociation of the GPI-AP. Importantly, two distinct chips run in parallel displayed very similar kinetics of capture and dissociation (Supplemental Fig. S4B).

Taken together, the findings obtained with isolated EV and total incubation medium from rat adipocytes demonstrate that chip-based sensing enables the sensitive identification of unprocessed GPI-AP in complex with phospholipids, as well as their differentiation according to the size of the releasing cell. In contrast, this differentiation was not feasible on the basis of the patterns of total proteins, total GPI-AP, or specific GPI-AP contained in adipocyte incubation medium (Supplemental Fig. S5).

Sensing of the Release of Unprocessed GPI-AP from Plasma Membranes In Vitro

Next, the putative release of unprocessed GPI-AP from adipocyte plasma membranes was studied in vitro using a “lab-on-the-chip” configuration. For this, plasma membranes were immobilized by hydrophobic interactions on the chip gold surface (2), which was reflected in the stepwise increases in phase shift with each injection (but only in the presence of Ca^{2+} for neutralization of negative surface charge) (Fig. 3, *period A*, blue vs. green curves). The incremental phase shifts decreased with the number of injections, compatible with a limited number of sites for immobilization. Only minor loss of the immobilized plasma membranes during multiple washing (buffer) cycles (*period A*) was observed as reflected in the small phase shift decreases. In the following, saturating

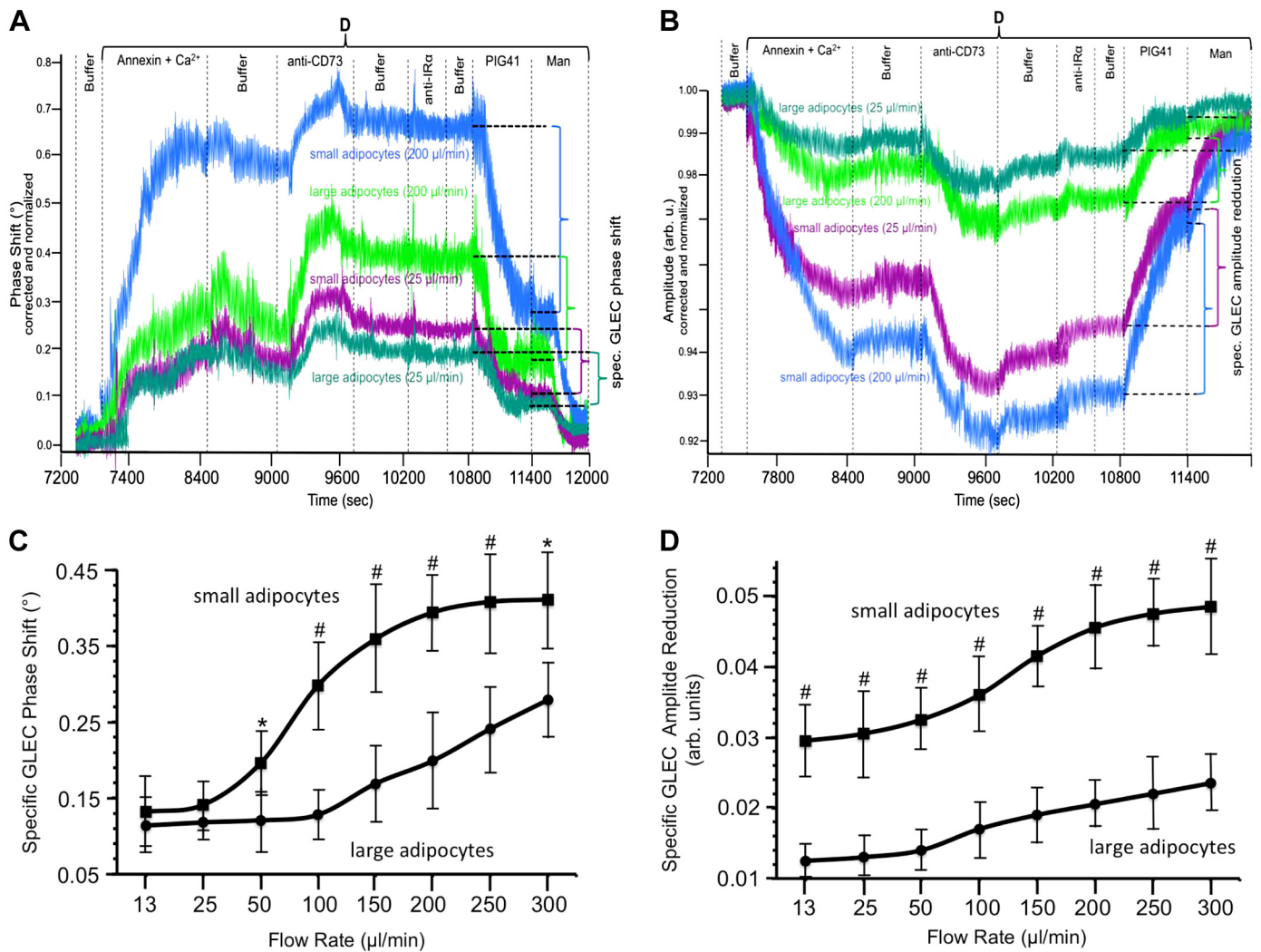


Fig. 4. Effect of flow rate and adipocyte size on the generation of unprocessed glycosylphosphatidylinositol-anchored proteins (GPI-AP) derived from plasma membranes. *A* and *B*: plasma membranes from small (blue and purple curves) or large (light green and dark green curves) adipocytes and Ca^{2+} were injected into α -toxin-coated channels for immobilization (see Fig. 2; *period A*). Unprocessed GPI-AP were generated from the immobilized plasma membranes by injection of 30 μM phosphoinositolglycan 37 (PIG37) at the flow rate indicated (*period B*). The plasma membranes were detached from the chip surface by the injection of glycine and EGTA (*period C*). Captured GPI-AP were detected by consecutive injections of annexin V, Ca^{2+} , anti-CD73 antibodies, and anti-insulin receptor α -chain (IR- α) antibodies, and finally by injection of PIG41 and mannose (Man; *period D*). For further details, see detailed protocols in data supplements. *C* and *D*: for quantitative evaluation, the experiment was performed with plasma membranes from small (squares) and large (circles) adipocytes, as described above, but, however, using increasing flow rates (13–300 $\mu\text{l}/\text{min}$) during *period B* (3,000–6,600 s). Specific phase shift (*C*) and amplitude reduction (*D*) induced by unprocessed GPI-AP (GLEC), as derived from three independent series of *periods A–D* were calculated as described (*A* and *B*) and are given as means \pm SD, with statistically significant differences between small and large adipocytes indicated. * $P < 0.05$ and # $P < 0.01$.

amounts of plasma membranes according to maximal phase shift were used for capture (*period A*) which ensured the comparison of roughly identical amounts of immobilized plasma membranes as putative source for unprocessed GPI-AP. The pronounced phase shift upon injection of anti-insulin receptor- α antibodies into the chip (Fig. 3A, end of *period A*) confirmed the immobilization of adipocyte plasma membranes, which typically express insulin receptor. The increases in phase shift upon sequential injections of plasma membranes and anti-insulin receptor- α antibodies did not significantly differ between small (Fig. 3A) and large (Fig. 3B) adipocytes (*period A*) confirming immobilization of similar amounts of membranes on the chip.

Unprocessed GPI-AP released from the immobilized plasma membranes during the subsequent injection of buffer were

captured by the α -toxin-coated chip in the presence of 30 μM PIG37 (Fig. 3, *period B*). This can be monitored only after almost complete elimination of the initial phase shift provoked by the immobilized plasma membranes, which is achieved by their detachment from the chip through deprotonization (pH 10), chelating of Ca^{2+} (EGTA), and final washing with buffer (*period C*). The stepwise increases in phase shift on sequential injection of annexin V and anti-CD73 antibodies, but not anti-insulin receptor- α antibodies, (*period D*) led to the detection of released and captured unprocessed GPI-AP (during *period B*) and demonstrated the subsequent quantitative removal of the plasma membranes (during *period C*). The specificity of capture and detection of the plasma membrane-derived GPI-AP was confirmed by final injection of 200 μM PIG41 (*period D*), which caused lowering of the phase shift by

roughly 70%. The remaining, apparently unspecific (i.e., not GPI-mediated) phase shift was completely abrogated by excess of mannose (*period D*). Therefore, only the portion competed for by PIG41 is regarded as GPI-AP-specific phase shift in the following.

Additional evidence for the specificity was provided by injection of PIG41 (turquoise curves) or mannose (yellow curves) immediately following detachment of the plasma membranes (Fig. 3, *period C*), as well as by use of “blank” chips lacking α -toxin (red curves), since each procedure completely prevented phase shift increase. Furthermore, injection of the detergent 4'-amino-7 β -benzamido-3 α , 12 α , 5 β -taurocholic acid (BATC; black and pink curves), which is known to preferentially solubilize GPI-AP vs. transmembrane proteins from eukaryotic plasma membranes (45), after detachment of the plasma membranes reduced the annexin V-induced phase shift increases in a concentration-dependent fashion (*period C*), but left unaltered those induced by anti-CD73 antibodies (*period D*). This suggests the exchange of phospholipids for BATC in the complexes with GPI-AP. Loss of phospholipids from the complexes was also achieved by bee venom PLA₂ (green curves), capable of cleaving off fatty acids from membrane-associated (glyco)phospholipids, including GPI. This treatment left captured GPI-AP with attached lysophosphatidate moiety only, which were detected by anti-CD73 antibodies, but not by annexin V. These data are compatible with the release of GPI-AP in complex with phospholipids from plasma membranes in vitro.

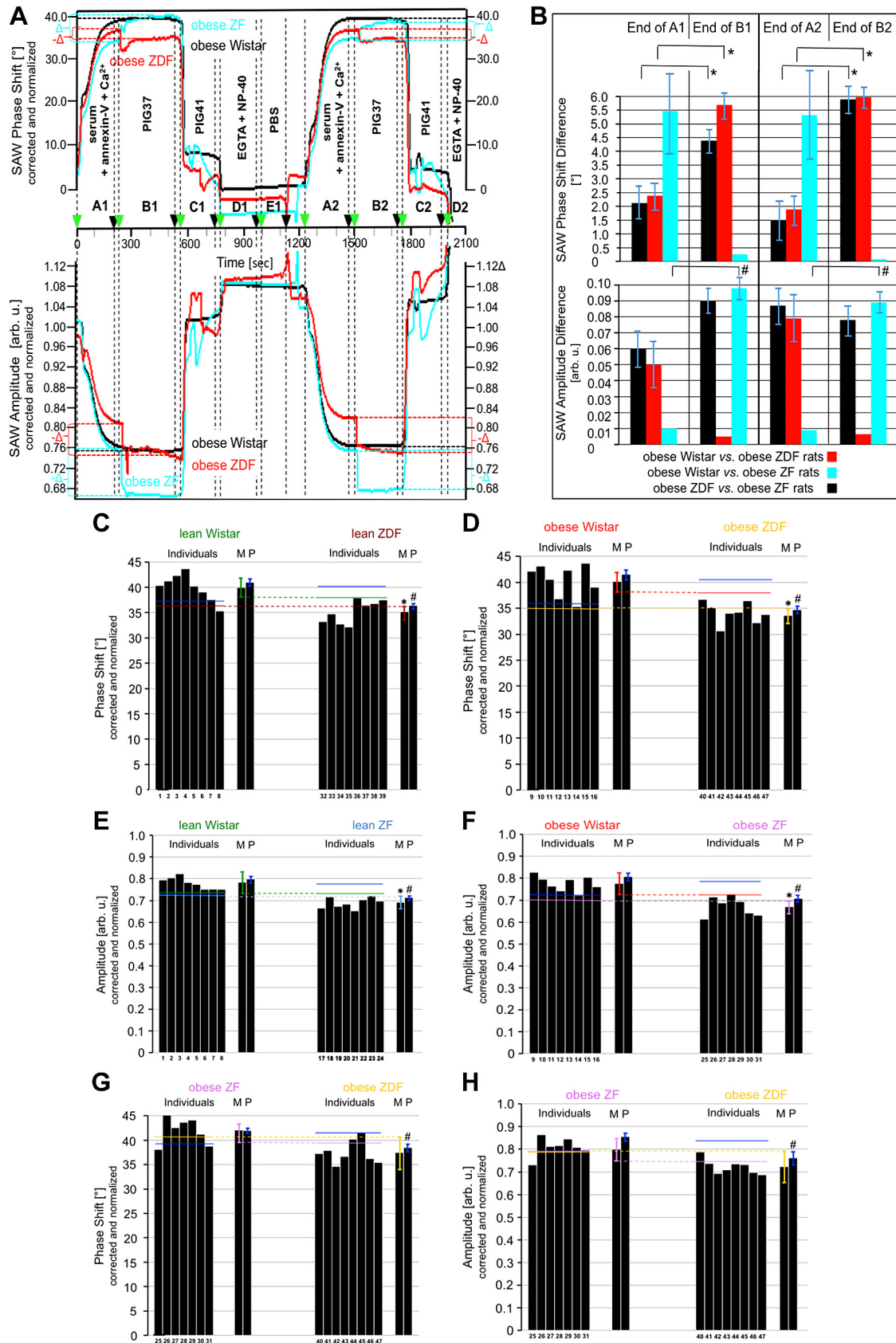
Interestingly, the phase shift increases (Fig. 3, blue curves) and amplitude reductions (data not shown) during annexin V and anti-CD73 antibody injections (*period D*) were considerably more pronounced for plasma membranes from small (Fig. 3A) compared with large adipocytes (Fig. 3B). The reduced phase shift and amplitude provoked by plasma membranes from large adipocytes vs. those from small ones is indicative for a lowered number, size, or specific mass (protein-to-lipid ratio) and higher viscosity (lipid-to-protein ratio), respectively, of complexes released from large vs. small adipocytes. So far the underlying molecular mechanism remains a matter of speculation. However, it is conceivable that high cholesterol lipid rafts are preferentially expressed at the plasma membranes of small adipocytes compared with those from large adipocytes due to a higher cholesterol-to-phospholipid ratio at the plasma membrane outer leaflet, with the consequence of release of complexes at elevated number, size, or specific mass

[see Supplemental Fig. S18 for a physiological and molecular explanation for the assumed inverse relationship between adipocyte size (and the blood glucose and insulin levels of the donor organisms as its relevant determinants) and cholesterol content of the plasma membrane outer leaflet]. Alternatively, the more pronounced membrane curvature of small vs. large adipocytes, possibly in combination with more prominent expression of high cholesterol lipid rafts, may favor the release of complexes from small compared with large adipocytes solely due to weakening of the hydrophobic interactions between membrane phospholipids and between those and GPI anchors.

Next the cellular and extrinsic factors that determine the efficacy of the release of unprocessed GPI-AP in vitro were investigated (Fig. 4). The release of the unprocessed GPI-AP turned out to be strongly dependent on the flow rate of the buffer injected during *period B* immediately after immobilization of the plasma membranes (*period A*) before their subsequent detachment from the chip (*period C*). This was reflected in considerably higher increases in phase shift (Fig. 4A) and reductions in amplitude (Fig. 4B) at 200 μ l/min (blue and light green curves) compared with 25 μ l/min (dark green and purple curves) for both small and large adipocytes during binding of annexin V and then of anti-CD73 antibodies during *period D*. The missing effect of injection of anti-IR α antibodies and the pronounced decline of phase shift and upregulation of amplitude in response to PIG41 argue for specific capture of unprocessed GPI-AP instead of typical transmembrane proteins. Apparently unprocessed GPI-AP were released from the plasma membranes of small adipocytes at high buffer flow with the highest efficacy. Interestingly, the amplitude reduction observed with large adipocytes at high flow rate was even lower than that induced by small adipocytes at low flow rate (Fig. 4B). In contrast, the more pronounced phase shift of small vs. large adipocytes was only observed when identical flow rates were compared (Fig. 4B). This may be explained by moderately elevated amount, specific mass, and size in concert with extensively elevated viscosity of the plasma membrane-derived GPI-AP, which become released from small compared with large adipocytes.

Quantitative analysis of the effect of the flow rate operative immediately after immobilization of the plasma membranes before the injection of annexin V and anti-CD73 antibodies on the release of plasma membrane-derived GPI-AP (Fig. 4) confirmed the positive correlation between flow rate and phase

Fig. 5. Chip-based sensing of unprocessed glycosylphosphatidylinositol-anchored proteins (GPI-AP) from rat serum. A: for phosphoinositolglycan 37 (PIG37)-dependent differentiation between obese Wistar, Zucker fatty (ZF), and Zucker diabetic fatty (ZDF) rats upon simultaneous capture and detection of GPI-AP, 40 μ l of pooled serum sample from obese Wistar (black curve), ZF (turquoise curve), and ZDF (red curve) rats, diluted fivefold with PBS and incubated with annexin V and Ca²⁺, were injected into α -toxin-coated channels (*period A1*). To initiate the differentiation, 30 μ M PIG37 were injected (*period B1*). The chips were regenerated by injection of PIG41 (*period C1*), and then EGTA and NP-40 (*period D1*), and finally PBS (*period E1*). To demonstrate reproducibility of this protocol, *periods A–D* were repeated under identical conditions with slightly adapted time frames. The maximal phase shift and minimal amplitude, respectively, measured after the injection of PIG37 at the end of *period B* are indicated as dashed lines. The differences in maximal phase shift and minimal amplitude are indicated between obese Wistar and ZDF rats (red Δ) and obese Wistar and ZF rats (turquoise Δ), as measured at the end of *periods B1* and *B2* (presence of PIG37), with Δ representing increases and $-\Delta$ decreases. B: the differences (absolute values) in phase shift ($^{\circ}$) and amplitude (arbitrary units) between obese Wistar and ZDF (red bars), obese Wistar and ZF (turquoise bars), and obese ZDF and ZF (black bars) rats measured at the end of *periods A1* and *A2* (absence of PIG37) or *periods B1* and *B2* (presence of PIG37) are given as means \pm SD. * $P \leq 0.05$. # $P \leq 0.01$. In the following experiments, the phase shift and amplitude were measured at the end of *period B*. C–H: for the comparative analysis of serum GPI-AP from rats of similar body weight and different genotype, phase shift (C, D, and G) and amplitude (E, F, and H) were measured in the presence of 30 μ M PIG37 as described for A and are given for the individual samples. The means (M) \pm SD, as well as the pooled samples (P) \pm SD, derived from 12 (M) and 4 (P) independent runs were calculated for each sample performed with one chip (reused six times) and 12/4 setting for each rat group. * $P \leq 0.05$. # $P \leq 0.01$. For further details, see detailed protocols in the data supplements. SAW, surface acoustic wave.



shift (Fig. 4C), as well as amplitude reduction (Fig. 4D), with the curves being shifted to the left and top, respectively, for small vs. large adipocytes. Together the findings hint to significantly higher susceptibility of plasma membranes from small compared with large adipocytes for release of unprocessed GPI-AP, dependent on the velocity of the buffer stream, as well as to significantly higher viscosity of those from small compared with large adipocytes.

Furthermore, on exposure of the immobilized adipocyte plasma membranes to detergent (BATC), extraction of fatty acids (BSA) or cholesterol (nystatin), and cleavage of lipidic membrane constituents [phosphatidylcholine (PC) specific-PLC, GPI-specific phospholipase D (GPI-PLD), PLA₂], led to altered phase shifts (Supplemental Fig. S6A) and amplitude reductions (Supplemental Fig. S6B) at variable degrees compatible with the presence of PC, GPI, fatty acids, and cholesterol in adipocyte plasma membrane-derived GPI-AP. Together, these findings argue for extrinsic “membrane-active” factors playing a role in the release of unprocessed GPI-AP among them and physiologically relevant cell surface tension, fluid flow rate, and serum albumin.

Implementation and Validation of the Sensing of Unprocessed GPI-AP in Serum

After successful demonstration of release of unprocessed GPI-AP from primary adipocytes into the incubation medium and their generation by isolated adipocyte plasma membranes in the “lab-on-the-chip” configuration, chip-based sensing was applied for their identification in serum of rats of different genotype and body weight (see Supplemental Table S2 for animal characteristics). Serum from lean Wistar rats provoked considerable and stable (in course of washing) increases in phase shift on capture by α -toxin-coated (Supplemental Fig. S7A, green curve) vs. “blank” (red curve) chips, as well as on subsequent sequential binding “in sandwich” of annexin V and anti-CD73 antibodies. However, with this experimental design differential responses for rats differing in both genotype and body weight were not obtained consistently (Supplemental Fig. S7B), for instance between lean Wistar and obese Zucker diabetic fatty (ZDF) rats. Importantly, a considerably diminished increase in phase shift (Supplemental Fig. 7C) for obese ZDF compared with lean Wistar rats or a more pronounced reduction in amplitude (Supplemental Fig. S7D) for obese Zucker fatty (ZF) compared with lean Wistar rats was achieved by addition of PIG37 in the midst of GPI-AP capture, which was maintained during subsequent phospholipid detection by annexin V binding and during washing. The PIG37-dependent difference in amplitude reduction as well as phase shift was found to be maximal with 30 μ M, as shown for serum from lean ZF vs. obese Wistar rats (Supplemental Fig. S7E) and lean ZDF vs. obese Wistar rats (Supplemental Fig. S7F), during repeated cycles of capture in the presence of increasing concentrations of PIG37, followed by phospholipid detection and complete displacement of the unprocessed GPI-AP from the chip by PIG41. Finally, to reduce the number of injection cycles, the capture and detection steps were combined (Supplemental Fig. S7G), which turned out to exert little effect on the serum-induced maximal increase in phase shift and reduction in amplitude compared with sequential injections of serum and annexin V.

Consequently, simultaneous injection of serum and annexin V for capture of the unprocessed GPI-AP and detection of the phospholipids (Fig. 5A, *periods A1* and *A2*), with subsequent measurement of phase shift and amplitude at the end of the injection of PIG37 (*periods B1* and *B2*) before regeneration of the chips (*periods C, D, and E*) was used as experimental protocol. It was most efficient for pairwise differentiation, as shown (Fig. 5A) for obese ZDF vs. obese ZF/Wistar rats (*top*) and obese ZF vs. obese ZDF/Wistar rats (*bottom*), with low variance between two consecutive cycles (*periods A1-D1* and *A2-D2*). Based on pairwise combinations, the differences in phase shift and amplitude between the serum samples were found to be significantly higher with lower variance when the measurements were performed after the PIG37 injection (Fig. 5B, end of *periods B1* and *B2*) compared with before (end of *periods A1* and *A2*). In conclusion, measurement of both phase shift and amplitude exerted in the presence of PIG37 is required for mutual differentiation of serum from rats of different genotypes with similar (obese) body weight. In addition, reuse of the chips after sequential displacement of the unprocessed GPI-AP using PIG41 (Fig. 5A, *periods C1* and *C2*), removal of phospholipids using NP-40 (*periods D1* and *D2*), and final washing (*period E*) turned out to be feasible, as manifested in nonsignificant deviations between *periods B1* and *B2*.

Differential Sensing of Unprocessed Serum GPI-AP in Normal, Diabetic, and Obese Rats

After determination of the sensitivity and linearity for chip-based sensing of unprocessed GPI-AP with regard to sample volume (Supplemental Fig. S8A) and of the variance (Supplemental Fig. S8B) between 1) the same channel (for reuse), 2) distinct channels of the same chip, and 3) distinct chips (Supplemental Fig. S8B), appropriate conditions (40- μ l sample volume, six reuses of the same channel) were used for the following measurements of individual and pooled serum samples of eight lean and obese Wistar, ZF, and ZDF rats covering different metabolic states (Supplemental Table S2) in pairwise comparisons between animals of different genotypes that are either lean or obese (Fig. 5, C–H and Supplemental Fig. S9) and vice versa between lean and obese animals that are of the same genotype (Supplemental Fig. S10, A–C).

In pairwise comparisons of either lean or obese rats, significant differences in phase shift and amplitude were observed for the means of the individually measured serum samples (M) between Wistar and ZDF (Fig. 5, C and D) or ZF (Fig. 5, E and F) rats. Between ZF and ZDF rats, trends were monitored only for the obese (Fig. 5, G and H), but not for the lean animals (Supplemental Fig. S9). In pairwise comparisons of rats of either Wistar (Supplemental Fig. S10A) or ZF (Supplemental Fig. S10B) or ZDF (Supplemental Fig. S10C) genotype, trends in phase shift and amplitude were measured for the means of the individual serum samples between lean and obese animals.

In conclusion, the means of the serum samples (M), as well as the values measured for the pooled samples (P) enabled the differentiation of individual rats for the majority of pairwise comparisons on the basis of phase shifts and amplitudes below or above the corresponding $M/P - 1 \times SD$ and $M/P + 1 \times SD$, respectively, determined for the counterpart rats (Fig. 6). The differences in phase shift and amplitude are more prominent for comparisons between rats (of similar body weight)

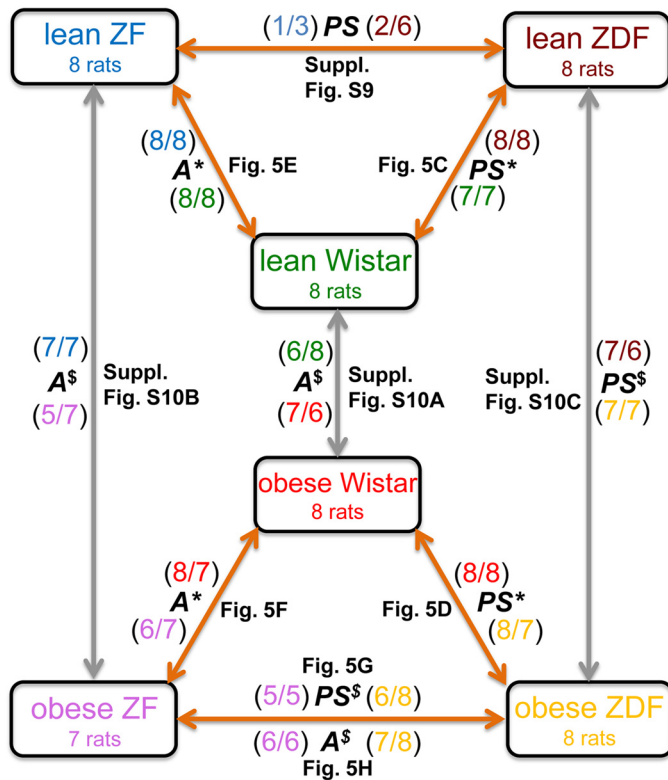


Fig. 6. Synopsis for the pairwise differentiation of rat sera by chip-based sensing. The arrows (brown for comparison of rats with different genotype and similar body weight; gray for different body weight and identical genotype) indicate the measurements of pairs of the different sera [eight samples each with the exception of seven for obese Zucker fatty (ZF) rats] with regard to maximal phase shift (PS) and minimal amplitude (A) as performed (see Fig. 4, C–H and Supplemental Fig. S11). Significant differences and trends between the means calculated from the individual serum samples (M) for a given pair are indicated as PS^* and A^* ($P \leq 0.01$) and $PS^{\$}$ and $A^{\$}$ ($P \leq 0.05$), respectively. The numbers (in color) indicate how many individual serum samples of a given rat group (marked in the same color) exhibit a maximal phase shift above and minimal amplitude below the corresponding means of the individual counterpart samples, M (first number), and the corresponding pooled sample, P (second number), respectively. ZDF, Zucker diabetic fatty.

differing in genotype (brown arrows) than for those between lean and obese rats (of identical genotype) (gray arrows). Importantly, repetition of this experiment using the same samples, but a distinct instrument, led to similar M and P values (Supplemental Table S3), which enabled differentiation of the rats according to genotype/body weight with comparable accuracy, as was true for the original instrument.

In agreement, differences in amplitude were observed between Wistar rats that had been subjected to bariatric or sham surgery and subsequently administered a (normal or vitamin supplemented) high-fat diet (66), reflecting the acquired lean and obese phenotype, respectively (Supplemental Table S4). Since significant differences in phase shift were measured neither between lean and obese Wistar rats (data not shown) nor between high-fat-diet-fed rats with bariatric and sham surgery (Supplemental Table S4), the amount, specific mass, or size of the complexes of unprocessed GPI-AP and phospholipids, which would be reflected in altered mass loading and thus phase shift, is presumably unaffected by the body weight.

Together, the data are compatible that hyperglycemia or hyperinsulinemia alone or in combination act as drivers for the release of unprocessed GPI-AP from donor cells into serum, which differ in specific mass, size, amount, and/or viscoelasticity, as can be monitored by SAW chip-based sensing. Remarkably, differences for unprocessed GPI-AP were measured between rats that did not display significant deviations in fasting glucose and plasma insulin levels (lean Wistar vs. lean ZDF, lean Wistar vs. lean ZF) (Fig. 6). These findings raise the possibility that unprocessed GPI-AP appear in serum before gross metabolic disturbances, which would make them particularly attractive for the prediction of T2D. Importantly, the differentiation apparently relies on the “configuration” between GPI-AP, phospholipids, and cholesterol in the complex, since chip-based sensing of GPI-AP alone (captured by α -toxin-coated chips without detection of phospholipids by annexin V binding), or detection of phospholipids alone (captured by annexin V-coated chips without detection of GPI-AP), or the presence of detergent in the sample did not support differentiation (data not shown).

Characterization of the Unprocessed GPI-AP in Rat Serum

Information about the biophysical nature of the serum complexes of unprocessed GPI-AP and phospholipids per se and differences herein between rats of different metabolic state was obtained by exposure of the pooled serum samples from eight rats to mechanical treatments before chip-based sensing (Fig. 7). With increasing numbers of freezing and thawing cycles, the differences in phase shift or amplitude between obese Wistar and Z(D)F rats considerably declined, dependent on the mode of sample handling (Fig. 7A). The “slow” mode led to significant loss of differentiation after a single cycle only, whereas the “rapid” mode did not significantly compromise differentiation during the initial two cycles. Incubation of the serum samples led to temperature-dependent declines in phase shift and amplitude differences, with significant and complete losses at 37°C and 65°C, respectively (Fig. 7B). Centrifugation of the serum samples led to drastic declines in phase shift and amplitude differences compared with the “routine” mode, dependent on the duration and centrifugal forces applied (Fig. 7C). Remarkably, centrifugation conditions (3,000 g, 10 min), which are insufficient for sedimentation of EV and thereby for their removal from the serum (supernatants analyzed), resulted in almost complete elimination of the differentiation between obese Wistar and Z(D)F rats. Ultrasonic treatment of the serum samples elicited dramatic reductions in phase shift and amplitude differences, as reflected in ~50% loss provoked by each cycle (Fig. 7D). Exposure of the serum samples to mechanical vibration caused reduction of phase shift and amplitude differences between obese Wistar and Z(D)F rats, dependent on the number of vibration cycles (Fig. 7E).

Two cycles of freezing and thawing (“slow” modus), incubation (42°C, 60 min), and centrifugation (3,000 g, 10 min), two cycles of ultrasonication, or two cycles of vibration (Fig. 7F) led to decreases of the serum-induced (open bars) phase shift and amplitude reduction by 50 to up to 90%, but exerted no or minor impairment only of the adipocyte medium-induced (hatched bars) as well as EV-induced (solid bars) reduction. Thus rat serum exhibits considerably higher sensitivity toward

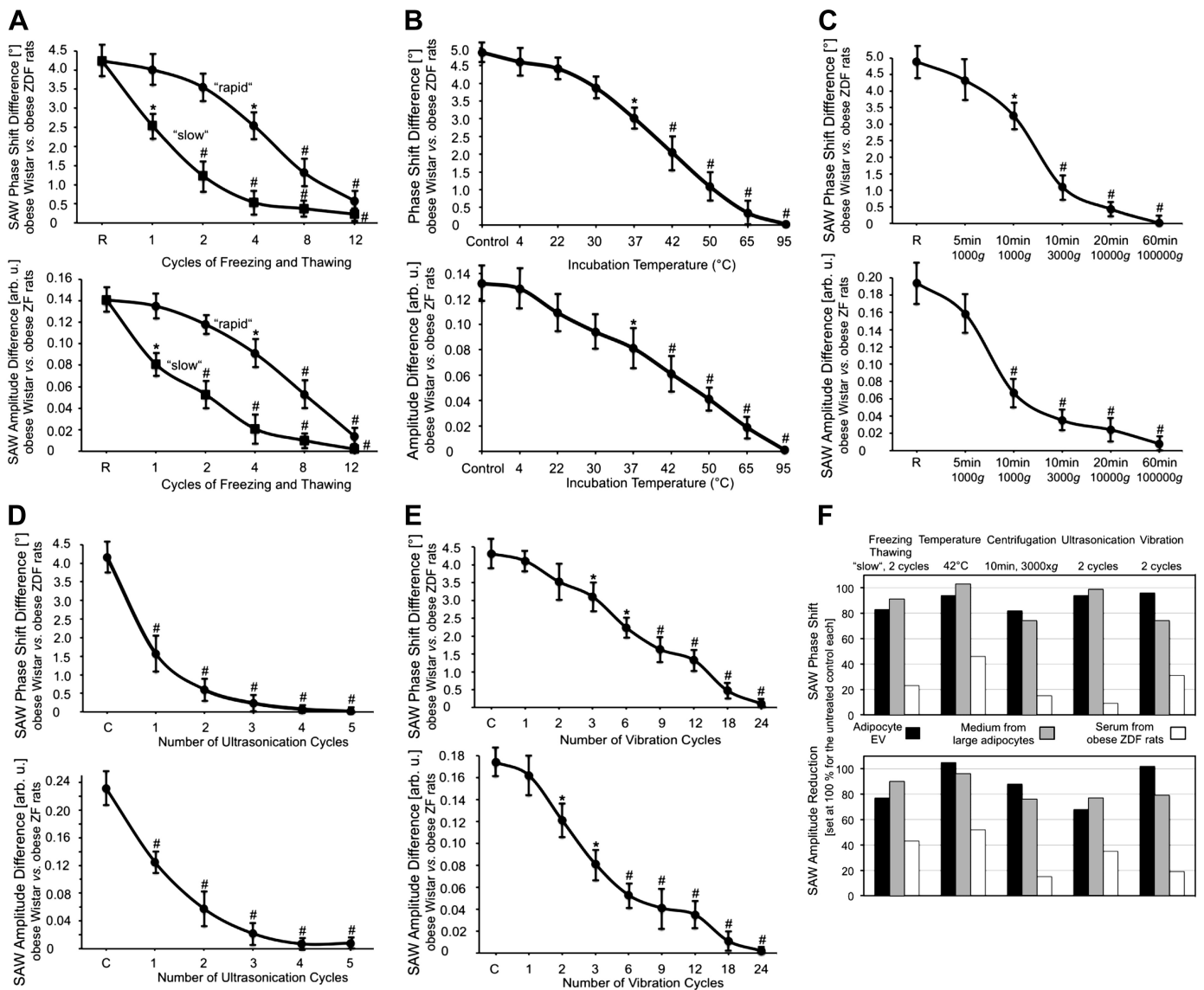


Fig. 7. Effect of physical treatments of unprocessed glycosylphosphatidylinositol-anchored proteins (GPI-AP) on their differentiation potential. The differences in the maximal phase shift and minimal amplitude between obese Wistar and Zucker diabetic fatty (ZDF) rats and between obese Wistar and Zucker fatty (ZF) rats, respectively, were measured (see Fig. 4A). A: effect of sample processing and storage. Serum samples were thawed and then subjected to the indicated numbers of freezing and thawing cycles in either "rapid" mode or "slow" mode or "routine mode" (R) before measurement. $*P \leq 0.05$ and $^{\#}P \leq 0.01$ vs. R. B: the effect of temperature. $*P \leq 0.05$ and $^{\#}P \leq 0.01$ vs. control. C: the effect of centrifugation. The supernatants were removed and immediately measured. $*P \leq 0.05$ and $^{\#}P \leq 0.01$ vs. R. D: the effect of ultrasonic waves vs. control (C). $*P \leq 0.05$ and $^{\#}P \leq 0.01$ vs. C. E: effect of vibration vs. C. $*P \leq 0.05$ and $^{\#}P \leq 0.01$ vs. C. Values are means \pm SD. F: putative similarities between unprocessed GPI-AP from different sources were investigated. Serum from obese ZDF rats, incubation medium of primary rat adipocytes of large size, and purified extracellular vesicles (EV) from large rat adipocytes were tested for their susceptibility toward physical treatments (see A–E) in comparison. For further details, see detailed protocols in data supplements. SAW, surface acoustic waves.

physical treatments compared with rat adipocyte medium and EV purified thereof. It is reasonable to assume that tissues/cells not identical with adipose/adipocytes are responsible for the release of rather labile (nonvesicular) complexes of unprocessed GPI-AP and phospholipids into serum, which mediate the differential effects on phase shift and amplitude between rats of different metabolic state. Rat serum may lack EV or harbor labile ones from nonadipocyte sources, such as macrophages, lymphocytes, and other immune cells, or the chip-based sensing may be biased for capture/detection of the complexes vs. EV due to methodological constraints or overwhelming expression of the former. The apparent exquisite

sensitivity of the complexes of unprocessed GPI-AP and phospholipids toward mechanical stress (Fig. 7) hints to a nonvesicular, possibly micelle-like, structure, held together by weak secondary interactions.

Information about the biophysical nature of the serum complexes of unprocessed GPI-AP and phospholipids per se and differences herein between rats of different metabolic state was obtained by evaluation of the effects of various enzymic and chemical treatments of serum on chip-based sensing. Removal of the GPI-AP coat by the GPI anchor-cleaving GPI-PLD suggested that differences in maximal phase shift and minimal amplitude between serum samples can be due to

changes in the relative abundance of the unprocessed GPI-AP vs. phospholipids and cholesterol (Supplemental Fig. S11). Furthermore, the differences in phase shift and amplitude for each of the pairwise comparisons of sera from metabolically different rats were reduced by 37–95% in the course of 1) removal of unprocessed GPI-AP from the sera by adsorption to microspheres coupled to α -toxin, 2) solubilization of lipidic structures with NP-40 (Supplemental Fig. S12A), 3) lipolytic cleavage of GPI-AP by (G)PI-specific PLC/PLD, and 4) degradation of phospholipids by PLA₂ (Supplemental Fig. S12, A and B) compared with the corresponding control treatments. These findings, together with the analysis of the effects of specific chemical and enzymatic treatments, which either cause degradation of the protein and anchor moieties of GPI-AP, or fail to do so (Supplemental Fig. S12C), are compatible with complexes of unprocessed GPI-AP and (phospho)lipids being responsible for the differentiation of rat sera by chip-based sensing.

In greater detail, depletion of the (c)AMP-degrading Gce1 and CD73 by adsorption to (c)AMP-agarose revealed that these GPI-AP seem to be constituents of complexes of high (lean Wistar rats) as well as low (obese ZDF rats) specific mass/size and elasticity, as reflected in the differences in phase and amplitude between treated and control serum samples (Supplemental Fig. S12D). These results, in combination with those from the evaluation of the effects of various detergents, known to induce solubilization of membrane proteins in general or of GPI-AP preferably (Supplemental Fig. S12E), as well as of cholesterol-depleting agents (Supplemental Table S5) on phase shift and amplitude differences between Z(D)F and Wistar rats, strongly suggest that the complexes, which provoked the differences in phase shift and amplitude between rat sera, as revealed by chip-based sensing, are constituted by unprocessed GPI-AP, among them Gce1 and CD73, phospholipids, and cholesterol.

In clinical practice, the measurement of a serum parameter for monitoring of disease states necessitates the delineation of a critical absolute threshold value to avoid the need for measurement of patient samples as relative differences to an appropriate “control,” as performed above with the pairwise comparisons of the rat sera and the calculation of differences in phase shift and amplitude (Fig. 5). “Controls” are often difficult to define and would lead to high expenditure for high throughput analysis. Consequently, for clinical practice, chip-based sensing of unprocessed GPI-AP in serum should provide absolute values for phase shift and amplitude.

The apparent mechanical lability, in particular toward vibration, of the rat serum complexes offered the possibility to correct by subtraction of the total values for noncomplex-mediated contributions (unaffected by vibration), which may be elicited by captured EV or lipolytically cleaved GPI-AP (Supplemental Fig. S13). Importantly, this procedure makes redundant the pairwise comparison of the serum samples (see Fig. 5). This protocol, together with the limited expenditure for preparation of the chips, which relies on 1) their regeneration and multiple use (by competitive displacement of the unprocessed GPI-AP from α -toxin rather than de-/renaturation of the capture molecule), 2) the reproducibility using distinct chips (Supplemental Fig. S8B) and instruments (Supplemental Table S3), and 3) the stability and ease of production of the capture molecule, in combination with knowledge about preparation and storage of (serum) samples (Fig. 7), may enable throughput chip-based

sensing of serum complexes in longitudinal studies to evaluate the possibility that their specific mass, size, amount, and/or viscoelasticity is diagnostic or predictive for the development of metabolic diseases.

Finally, the criterion of physical lability was used to investigate whether the rat serum complexes, as measured by chip-based sensing, and the rat adipocyte plasma membrane-derived complexes, as generated by the “lab-on-the-chip,” are related (Fig. 8). In fact, exposure of “lab-on-the-chips” with captured complexes (during *period B*) to vibration (pink and brown curves) and ultrasonication (yellow and turquoise curves) after removal from the instrument (*period C*) considerably reduced the phase shift increases (Fig. 8A) and amplitude reductions (Fig. 8B) provoked by injection of annexin V compared with control (blue and green curves), as was true for the serum complexes (Fig. 8, D and E). In contrast, the mechanical forces exerted only minor impairments on the binding of anti-CD73 antibodies, indicating that the capture of GPI-AP per se remained unaffected. These findings argue for structural similarity between the complexes consisting of unprocessed GPI-AP and lipids released from rat adipocyte plasma membranes and those present in rat serum.

In addition to mechanical forces (e.g., buffer flow) and “membrane-active” agents in the buffer (e.g., detergents, enzymes, albumin), the metabolic state of the rats as the donors for the adipocyte plasma membranes critically determines the release of complexes in the “lab-on-the-chip” (Supplemental Fig. S14). In fact, using adipocyte plasma membranes for phase-shift measurement, it was feasible to differentiate between old and obese Wistar rats of similar body weight (Supplemental Fig. S14A). Furthermore, the presence of BSA during this release (Supplemental Fig. S15) led to significant increases in the differences in specific phase shift (Supplemental Fig. S15A) and amplitude reduction (Supplemental Fig. S15B) for total adipocytes from obese vs. lean ZDF rats, as well as for small adipocytes from young vs. large adipocytes from old Wistar rats. On the basis of the data obtained with the chip-based sensing in vitro (isolated plasma membranes and primary adipocytes) and in vivo (serum), it is tempting to speculate that, in vivo, 1) release of complexes of unprocessed GPI-AP and lipids with regard to specific mass, size, amount, and viscoelasticity is determined by the extracellular fluid (e.g., blood pressure, albumin, fatty acids) and the metabolic state of the releasing cells; and 2) plasma membranes of adipocytes can operate as the source for the serum complexes. However, the abundance of adipocyte-derived complexes in serum remains to be investigated.

Sensing of Unprocessed GPI-AP in Human Serum

Finally, the possibility of expression of unprocessed GPI-AP in human serum was tested by chip-based sensing (Fig. 9). Sequential injection of a pooled (Fig. 9A) or individual (Fig. 9B) human serum sample (*period A0*), annexin V in the presence of Ca²⁺ (*period A1*), and anti-CD73 antibodies (*period B*) into α -toxin-coated channels elicited considerable increases in phase shift (Fig. 9A) and reductions in amplitude (Fig. 9B), which each resisted subsequent washing (controls). In contrast, only very minor effects on phase shift and amplitude were observed with “blank” channels (data not shown). The annexin V/Ca²⁺-induced, but hardly the serum- and anti-

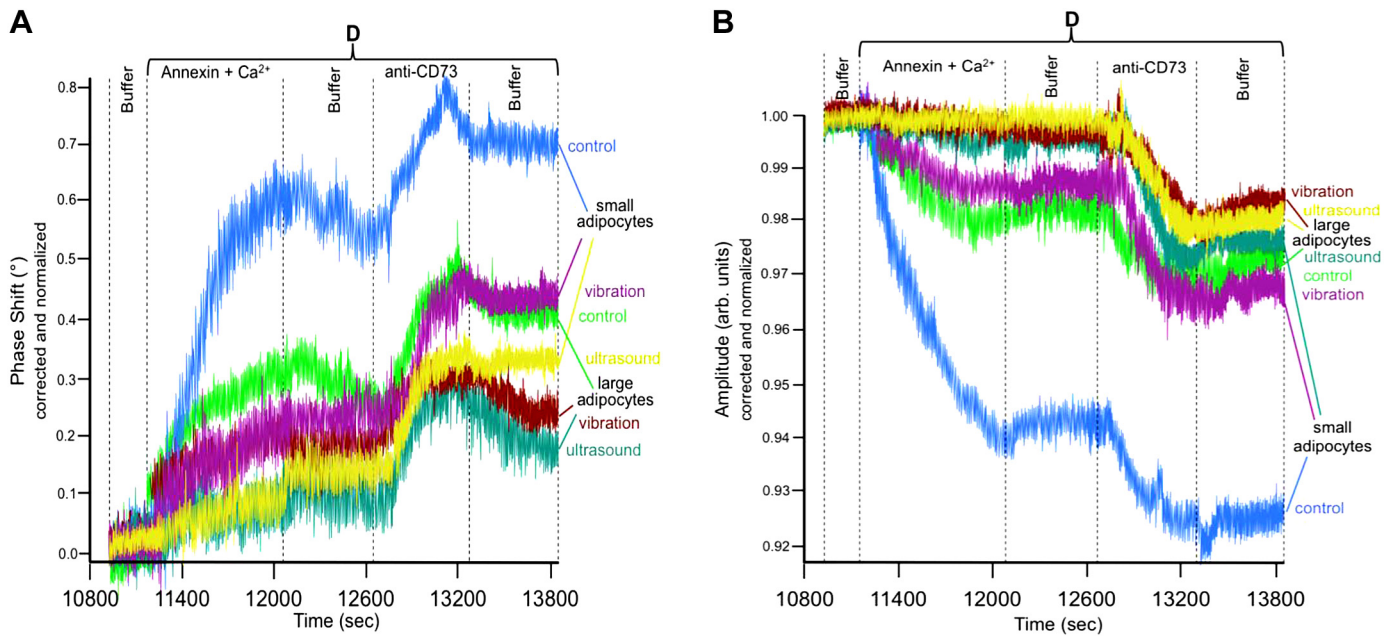


Fig. 8. Characterization of unprocessed glycosylphosphatidylinositol-anchored proteins (GPI-AP) derived from rat adipocyte plasma membranes. The experiment was performed with plasma membranes from small and large adipocytes, as described for Fig. 3. At the end of *period B*, the chips were removed from the instrument without emptying of the channels and put into sealed and fitted plastic chambers. Chips with captured GPI-AP were exposed to vibration or ultrasound treatment. Other chips were left untreated as controls. *Period D* is shown only. *A*: phase shift. *B*: amplitude. For further details, see detailed protocols in data supplements.

CD73-induced, upregulations of phase shift and amplitude reduction were abrogated by EGTA and PLA₂ (but not by PC-PLC), demonstrating the specific detection of phosphatidylserine in complex with GPI-AP by annexin V. The specific capture of the unprocessed GPI-AP was confirmed by drastically diminished upregulations of phase shift (Fig. 9A) and amplitude reduction (Fig. 9B) compared with control with serum which had been depleted of GPI-AP by adsorption to α -toxin-coupled microspheres before injection, or the inclusion of PIG41 during the injection. This was even more pronounced after solubilization of the samples with the detergent BATC before injection, which is compatible with formation of labile complexes between phospholipids, cholesterol, and GPI-AP. The presence of unprocessed GPI-AP was confirmed by reductions in the phase-shift increase (Fig. 9A) and amplitude reduction (Fig. 9B) by 80–90% in course of enzymic (PI-PLC or GPI-PLD) and chemical (hydrogen fluoride dephosphorylation or nitrous deamination) pretreatments, which all are

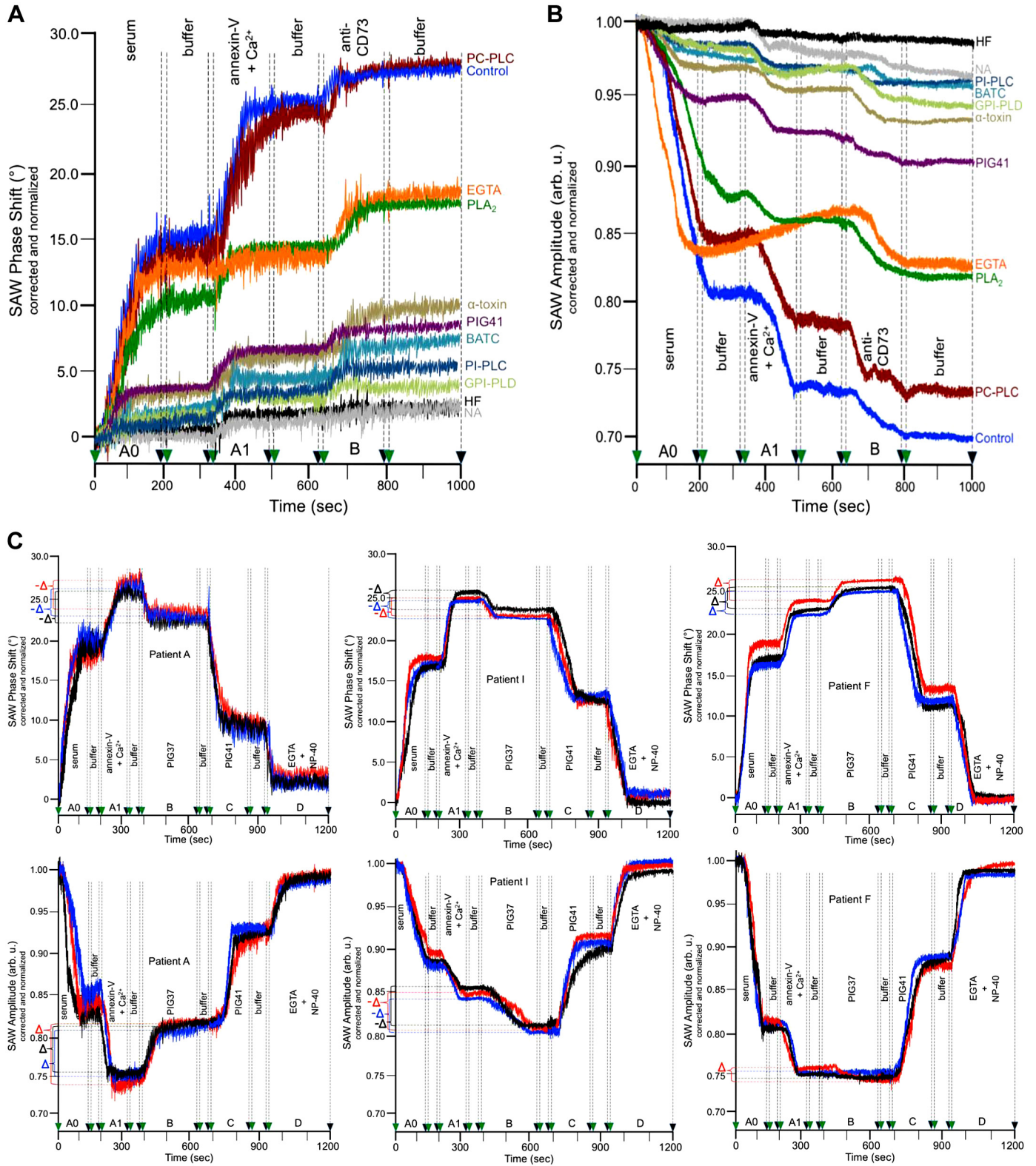
known to specifically cleave within the phospholipid or core glycan portions of GPI-AP.

The analysis of fresh unfrozen serum from 10 probands (for proband characteristics, see Supplemental Table S6) revealed clear-cut similarities in the kinetics of phase shift and amplitude changes, i.e., shapes of the corresponding curves, for the periods of both capture of the GPI-AP and detection of the complexes (Fig. 9C and Supplemental Fig. S16). However, in contrast to the observed correlation between the genotype/body weight of rats and the PIG37-dependent alterations in phase shift and amplitude during chip-based sensing of unprocessed GPI-AP in their serum, no consistent differences were identified between control *subject A* and an overweight (I) and obese (F) T2D patient based on the protocol for pooled human serum samples, even in the presence of PIG37 during time-resolved capture for maximal differentiation (Fig. 9C). The same held true for the inclusion of overweight and obese type 1 diabetes patients (Supplemental Fig. S16).

Fig. 9. Characterization of unprocessed glycosylphosphatidylinositol-anchored proteins (GPI-AP) present in human serum. Pooled (A) or individual (B) serum samples from normal probands were injected into α -toxin-coated or “blank” channels (*period A0*). Before the injection, the samples were kept untreated (control) or treated as indicated. To demonstrate stable capture of unprocessed GPI-AP, running buffer was injected. Thereafter, annexin V and Ca²⁺ were injected (*period A1*). To demonstrate stable detection of unprocessed GPI-AP, running buffer was injected. Thereafter, anti-CD73 antibodies were injected (*period B*). To demonstrate stable detection of GPI-AP “in sandwich,” running buffer was injected. For further details, see data supplements. *C*: for phosphoinositolglycan 37 (PIG37)-dependent sensing of unprocessed GPI-AP in serum of control subjects and diabetic patients, pooled serum samples were injected into α -toxin-coated or “blank” channels (*period A0*). Following washing, annexin V and Ca²⁺ were injected (*period A1*). After rinsing of the channels and injection of 30 μ M PIG37 (*period B*) and then running buffer, the chips were regenerated by injection of 200 μ M PIG41 (*period C*), then of running buffer, and finally of EGTA and NP-40 (*period D*). The maximal phase shifts and minimal amplitudes, respectively, measured at the end of the consecutive injection of annexin V + Ca²⁺ (*period A1*) and PIG37 (*period B*) are indicated as dotted lines. These PIG37-dependent changes in phase shift and amplitude are marked by triangles for each serum sample. Δ and $-\Delta$ indicates increase and decrease of phase shift or amplitude, respectively, in comparison to the absence of PIG37 (i.e., difference between end of *period B* and *A1*). For further details, see detailed protocols in data supplements. BATC, 4'-amino-7 β -bezamido-3 α , 12 α , 5 β -taurocholic acid; GPI-PLD, GPI-specific phospholipase D; HF, hydrogen fluoride; NA, nitrous acid; PC-PLC, phosphatidylcholine-specific-phospholipase C; PI-PLC, phosphatidylinositol-specific phospholipase C; SAW, surface acoustic waves.

Information about the physical stability of the complexes of GPI-AP and lipids in human serum per se and differences herein between humans and rats were obtained by exposure of the sera to mechanical treatments before measurement (Fig. 10), which revealed that conditions that caused significant

lowering of the changes in PIG37-dependent phase shift and amplitude provoked by the serum complexes from rats exerted only (very) minor (centrifugation, ultrasonication) or no effects at all (freezing plus thawing, elevated temperature) on those from humans. With the human complexes, marked declines to



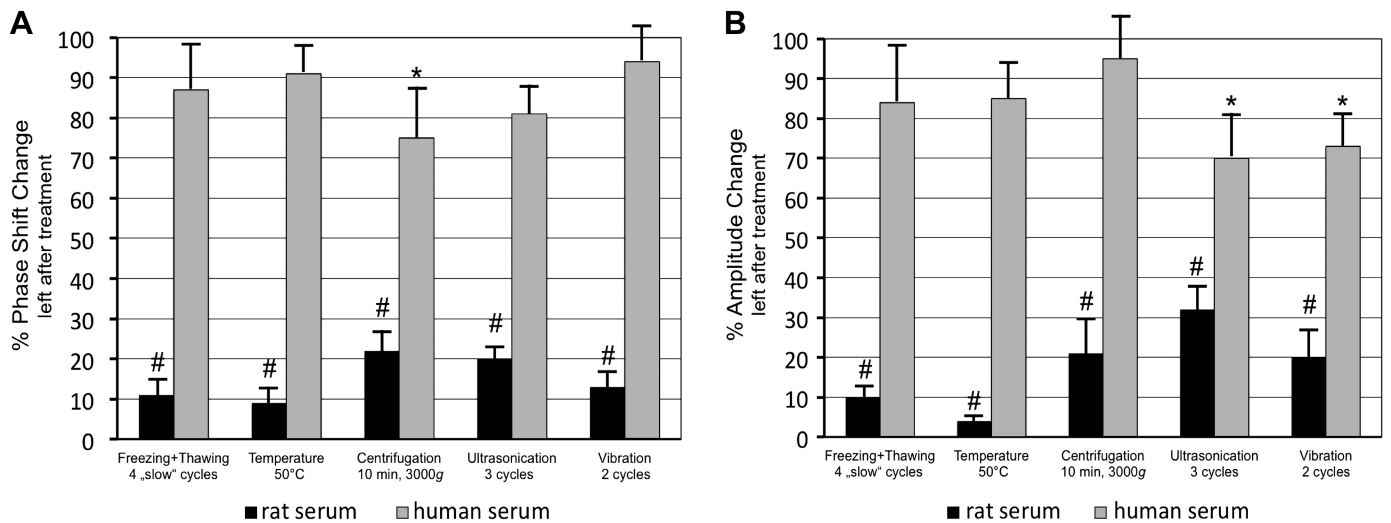


Fig. 10. Comparison of the susceptibility of the unprocessed glycosylphosphatidylinositol-anchored proteins (GPI-AP) toward physical treatments between rat and human serum. The relative effects of the various physical treatments of rat (solid bars) and human (shaded bars) sera under the specific conditions indicated on the phosphoinositolglycan 37 (PIG37)-dependent changes in phase shift (A) and amplitude (B), performed as described (Supplemental Figs. S15 and S20) for the frozen rat and fresh human serum samples, are given as %change remaining left compared with control (set at 100%). Values are means \pm SD. * $P \leq 0.05$ and # $P \leq 0.01$ vs. control, for each treatment.

up to complete abrogation of the PIG37-dependent changes in phase shift and amplitude were observed only under the most extreme conditions for each treatment (Supplemental Fig. S17). Thus complexes of human serum exhibited considerably higher stability toward mechanical stress compared with the rat complexes, which prevented the determination of threshold values for specific complex-induced phase shift and amplitude, as is feasible for rats (see Supplemental Fig. S13).

Taken together, the presence of unprocessed GPI-AP in complex with lipids in human serum, which display similar composition and structure as their rat counterparts, was unequivocally demonstrated. Their apparent noncorrelation with the metabolic state in humans could be explained by 1) non-coupling of metabolic stress and complex release from donor cells and/or complex degradation by serum GPI-PLD; 2) varying physical stability with the most labile complexes being correlated to the metabolic state but prone to disruption or loss during serum sample collection, preparation, and/or sensing, even if handled in the unfrozen state (as was the case for the tested human serum samples, which may have lost the correlative labile complexes and contain only the metabolically irrelevant stable ones); and 3) the number of analyzed samples being inadequate for the elucidation of patterns for chip-based sensing of serum complexes from metabolically differing probands. Thus it cannot be excluded that, in human serum, subpopulations of complexes of GPI-AP and lipids are expressed that correlate with the metabolic state, but are of lower stability compared with the rat complexes (and the human complexes measured in the present study) and become lost during the sample processing procedures, as used here.

For detection of GPI-AP harboring the glycan core by chip-based sensing, its detection limit measured with chip-based sensing using detergent-solubilized AChE under standard conditions (α -toxin-coated chips, 40 μ l sample volume) of 0.3 mg/ml would necessitate that $\sim 0.5\%$ of the total proteins in mammalian plasma (typically 60–80 mg/ml) is constituted

by GPI-AP. This certainly represents a rather high and presumably unrealistic portion. However, it was unexpectedly found that 2 μ l of serum from normal rats elicit the same phase shift of 0.2° (as the lower detection limit) as 12 μ g of detergent-solubilized AChE. With a calculated concentration of 100 μ M, GPI-AP would account for even up to 10% of total plasma proteins. This is in striking contrast to the broadly documented plasma proteome with albumin and globulins accounting for $>98\%$.

Importantly, on treatment of the serum with excessive amounts of PI-PLC (*Bacillus thuringiensis*; 3 units/ml, 60 min, 30°C) for quantitative cleavage of the GPI anchor, 200 μ l were required for the induction of 0.2° phase shift corresponding to 4.8 μ g of lipolytically cleaved AChE. With a calculated concentration of 0.40 μ M, GPI-AP would account for only 0.04% of the total plasma proteins. The drastic difference in the calculated contribution to the plasma proteome between unprocessed (by detergent or PI-PLC) and lipolytically cleaved GPI-AP may be explained best by a tremendous improvement in sensitivity of the chip-based sensing for the former due to complex formation with lipids and other proteins, leading to amplification of the phase shift by the increased mass and/or size loading onto the chip surface. Thus, under standard conditions (40 μ l), GPI-AP become detectable by chip-based sensing only, if they were expressed in complexes.

Qualitatively similar results were obtained with serum from healthy subjects. However, the fivefold higher sample volume required for the induction of 0.2° phase shift and the small difference between the unprocessed and the lipolytically cleaved samples may indicate that, in contrast to the rat complexes, a considerable portion of the complexes was already dissociated in the human serum samples before chip-based sensing, with the consequence of lowered sensitivity of detection of unprocessed GPI-AP.

On the basis of the available data, it is reasonable to assume that unprocessed GPI-AP in complex with lipids comprise between 0.01 and 0.1% of the plasma proteome at a concen-

tration of 10–100 nM. For a more accurate determination, calibration of the chip-based sensing with the authentic complexes instead of detergent-solubilized AChE as standard is required. However, isolation of the complexes will be a formidable task due to their lability, as demonstrated here. Taken together, chip-based sensing enables the detection of serum complexes of unprocessed GPI-AP and lipids, which are correlated to the metabolic state, rather than of monomeric (unprocessed or lipolytically cleaved) GPI-AP, which can be measured by RIA and ELISA with considerably higher sensitivity (31), but do not have predictive value.

DISCUSSION

The presence of the GPI anchor at a GPI-AP per se appears to confer some important behavioral and functional attributes onto the protein moieties to which it is attached (39, 41, 49), such as high lateral mobility of GPI-AP within the plane of the extracellular plasma membrane leaflet, and preferred association and oligomerization within specific cholesterol-harboring membrane microdomains, such as lipid rafts (26, 33, 53, 57, 59, 60, 62, 67). In adipocytes, which are specifically devoted to glucose and lipid metabolism, plasma membrane lipid rafts of higher and lower cholesterol content can be discriminated from one another (42, 47) with the GPI-AP, Gce1, and CD73, moving from the former to the latter lipid rafts in a signal-dependent fashion (43, 44). Clustering in lipid rafts may be responsible for weaker association of GPI-AP with plasma membranes compared with transmembrane proteins and thereby facilitate release from the cell surface of GPI-AP with the unprocessed GPI anchor remaining attached in complex with lipids (cholesterol, phospholipids) and in positive correlation to the cholesterol content of the lipid rafts.

The data presented strongly argue for the expression of complexes consisting of unprocessed GPI-AP and lipids (phospholipids, GPI lipids, cholesterol) in rat and human serum, which closely resemble those derived from adipocyte plasma membranes in a “lab-on-the-chip” configuration, but are clearly different from EVs, and have not been reported so far. The presence of phosphatidylserine as a (presumably one and minor) phospholipidic constituent of the complexes, which is prerequisite for their sensing, with high sensitivity in the sandwich configuration by a commercially available phospholipid-binding protein, may be regarded as surprising on the basis of the known enrichment of sphingolipids and PC, as well as the low concentration of phosphatidylserine at the outer membrane leaflet of lipid rafts (71). However, recent studies have demonstrated the expression and functional role of phosphatidylserine at lipid rafts of mammalian plasma membranes. Phosphatidylserine promotes the formation of lipid rafts and low-density liquid-ordered microdomains in physical models of the plasma membranes (22), as well as in plasma membranes of living cells (6), consisting of areas of sphingomyelin in the outer leaflet and PC in concert with phosphatidylserine in the inner leaflet (61). Remarkably, the phospholipid distribution between liquid-ordered raft and liquid-disordered non-raft domains was shown to depend on the method of their isolation, but, with both the detergent-free and the detergent method, phosphatidylserine was recovered with lipid rafts, albeit at rather low concentrations (21). Of greatest relevance may be the finding that phosphatidylserine is released from

lipid rafts of platelets in EV exposing it at the outer membrane leaflet (74). Together, these findings are compatible with phosphatidylserine located at lipid rafts as a minor species being involved in the formation of complexes of GPI-AP, cholesterol, and phospholipids, among them phosphatidylserine. Certainly, the expression of sphingolipids and other phospholipid species, such as PC, at the complexes as the major lipid constituents remains to be studied by (lipidomic) methods that are not biased toward phosphatidylserine, as is chip-based sensing. In any case, the unequivocal detection of (presumably low) amounts of phosphatidylserine in complex with GPI-AP demonstrates the exquisite sensitivity of the chip-based sensing, which is due to amplification of the phase shift and amplitude signals in the course of binding in sandwich of annexin V.

The identification of these complexes, furthermore, verifies the initial hypothesis that GPI-AP, as the most amphiphilic constituent of the eukaryotic plasma membranes, are not as stably embedded as is true for typical transmembrane proteins, cholesterol, and phospholipids. They are, however, released as unprocessed entities, i.e., in the absence of (the well-documented) proteolytic and lipolytic processing, in a spontaneous or controlled fashion into extracellular fluids (incubation medium, blood) in response to the (patho)physiological state of the donor cell/organism, as reflected here in the dependence on the rat adipocyte size and rat genotype (diabetic)/body weight (obese), as well as to extrinsic factors, as reflected here in the impact of the composition of the extracellular fluid (albumin, flow rate). As a practical consequence, chip-based sensing of unprocessed GPI-AP in complex with lipids may be used to test plasma membranes and surfaces of cells of interest *in vitro* and *in vivo* for their intrinsic (biophysical/chemical) stability or susceptibility toward cellular/extrinsic stress factors. The possibility that the appearance and biophysical characteristics of these complexes are indicative or even predictive for certain stress-associated diseases, such as hyperinsulinemic and hyperglycemic states during the pathogenesis of T2D (Supplemental Table S7), deserves further investigation. This preferably should rely on longitudinal studies with adequate sample size and on an improved protocol for serum preparation, transfer, and processing to bypass the putative loss of the apparently extremely labile but stress-related human complexes.

We suggest the following hypothetical model for the release of unprocessed GPI-AP into blood (Supplemental Fig. S18): In the normoinsulinemic normoglycemic state, the expression of high cholesterol lipid rafts favors the release of unprocessed GPI-AP. Several configurations of the constituents within the complexes of GPI-AP and lipids and releasing mechanisms are conceivable (see legend to Supplemental Fig. S18). The membrane rigidity at high cholesterol lipid rafts may control the rate of the spontaneous as well as controlled release of the unprocessed GPI-AP in a positive fashion, either through stabilization and extrusion of “open sheets” or through facilitation of the shaping of “closed” micelles. Detection of unprocessed GPI-AP in serum from normal rats by chip-based sensing, in comparison to buffer alone, reveals 1) a pronounced SAW phase shift due to capture of complexes of GPI-AP and lipids with a certain specific mass and size at a certain number; and 2) a small reduction in the SAW amplitude, only, due to capture of complexes of high elasticity and low viscosity. In

the hyperinsulinemic (hyperglycemic) state, low cholesterol lipid rafts formed from the high cholesterol lipid rafts through cholesterol deprivation, release of complexes of GPI-AP, and lipids of reduced specific mass and size and/or at reduced number. Detection of unprocessed GPI-AP in serum of hyperinsulinemic rats by chip-based sensing in comparison with buffer alone reveals 1) a small SAW phase shift only due to capture of complexes of GPI-AP and lipids with reduced specific mass and size and/or at diminished number; and 2) a pronounced reduction in SAW amplitude due to capture of complexes of low elasticity and high viscosity. Serum from hyperinsulinemic rats exhibits the considerably reduced phase shift due to downregulated specific mass, size, and/or number, in parallel to the diminished amplitude due to elevated viscosity of complexes with incomplete GPI-AP coat compared with serum from normoinsulinemic rats due to large complexes with complete GPI-AP coat.

It is tempting to speculate that the observed reductions in number, size, or specific mass, as reflected in decreased phase shift and amplitude, of serum complexes from hyperinsulinemic hyperglycemic rats compared with normoinsulinemic normoglycemic ones (Fig. 5, 6) and in complexes released from plasma membranes *in vitro* of small compared with large rat adipocytes (Fig. 3) are causally linked with the common underlying molecular basis of high cholesterol lipid rafts or high membrane curvature supporting release of the complexes. In any case, the apparently diminished release of unprocessed GPI-AP in complex with lipids from donor cells of insulin-resistant obese rats *in vivo* and from adipocyte plasma membranes of old rats *in vitro* suggests that the size of the donor cells is critical for release of the complexes, and that the parameters of the plasma membranes that define the releasing efficacy can be studied *in vitro* by the chip-based sensing.

Complexes of unprocessed GPI-AP and lipids are thought to be remodeled and degraded in blood during a multistep process initiated by lipolytic separation of the protein moiety-glycan core and phosphatidate residue of the GPI-AP by serum GPI-PLD. *In vitro* GPI-PLD action necessitates presentation of the GPI-AP within detergent micelles (23, 65). In blood, this requirement may be met by complexes of GPI-AP and lipids, since serum complexes in the absence of exogenous detergent represent substrates for GPI-PLD *in vitro*, as shown here. Assuming low activity of GPI-PLD in the normoinsulinemic normoglycemic state, the GPI-AP coat of the complexes becomes degraded slowly only (Supplemental Fig. S18A, thin arrow). Efficient release, in concert with low degradation, is responsible for the appearance of complexes at high number and of high specific mass and large size with an extended, uniform, and rigid GPI-AP coat of high elasticity in the serum from normal rats (Supplemental Fig. S18A).

Assuming high activity of GPI-PLD in the hyperinsulinemic (hyperglycemic) state, the GPI-AP coat of the complexes becomes intensely degraded (Supplemental Fig. S18B, thick arrow). Extensive shaving of the GPI-AP coat from the surface of the complexes would also provide an explanation for the seemingly contradictory decline in amplitude in parallel with the decrease in phase shift in the course of development of the hyperinsulinemic (hyperglycemic) state. Typically, a portion of the amplitude reduction can be attributed to the mere capture of the complexes of GPI-AP and lipids, since mass loading per se will cause dampening of the SAW amplitude. More impor-

tantly, the viscoelasticity of the complexes is presumably determined by the GPI-AP coat with the less extended and intact, the lower/higher the elasticity/viscosity of the complexes and the higher the amplitude reduction provoked by energy absorption through the viscous complexes. Consequently, hyperactivation of serum GPI-PLD in hyperinsulinemic (hyperglycemic) rats will foster complex-induced amplitude reduction compared with the elastic complexes with intact GPI-AP coat from normal serum.

The parallel decline in amplitude (i.e., elasticity of the complexes) and phase shift (i.e., specific mass/size/amount of the complexes) when measuring serum from hyperinsulinemic (hyperglycemic) vs. normal rats could be explained solely by elevated activity of serum GPI-PLD. In agreement, treatment of serum samples with GPI-PLD resulted in drastic and parallel declines in both phase shift and amplitude up to concentrations that interfered with capture due to complete elimination of the GPI-AP (see Supplemental Fig. S11). It would be interesting to determine whether the SNP in the GPI-PLD gene found associated with T2D patients in a recent genomewide association study (73) is correlated with an increase in the amount and/or specific activity of GPI-PLD.

Complexes partially digested with GPI-PLD, as may be generated in serum from hyperinsulinemic (hyperglycemic) rats, are presumably of heterogeneous nature differing in the relative portions of complete GPI-AP, cholesterol and phospholipids and, in consequence, in specific mass, size and viscoelasticity. Analysis of these parameters is not possible with classical biochemical methods or necessitates pre-fractionation steps which are difficult to perform due to the inherent instability of the complexes. Moreover, changes in the expression of certain GPI-AP and phospholipids in plasma, as measured by ELISA (for CD59), proteomics and lipidomics (31), have been described for aging (75), breast cancer (10) and Alzheimer disease (8), respectively. However, changes in the GPI-AP-to-cholesterol-to-phospholipid ratio of complexes with corresponding insults on their biophysical characteristics, which may correlate to the (patho)physiology of the releasing cell/organism, will escape detection by "single-parameter" methods, such as mass spectrometry.

The question may be raised whether out of the total GPI-AP found in serum, specific ones are related to specific disease states. Answering of this question would have required the analysis of a few selected GPI-AP rather than the total set of GPI-AP. However, it remains doubtful whether certain diseases are associated with the release of certain (unprocessed) GPI-AP into the blood of patients. Vice versa, the chip-based sensing was designed to monitor the release of the total unprocessed GPI-AP, irrespective of the nature of their protein portion. The underlying rationale relied on the working hypothesis that the release of GPI-AP with complete anchor (in complex with lipids) should be determined almost exclusively by the interplay of the GPI anchors and the donor membranes and not be affected by the protein portion of the GPI-AP. Accordingly, specific disease states should correlate with changes in the appearance in blood of unprocessed GPI-AP in total rather than of a specific GPI-AP harboring a protein moiety with disease-related function.

Finally, the use of α -toxin-coated chips with omission of subsequent phospholipid detection (by annexin V binding) may also be useful for the identification of lipolytically cleaved

soluble versions of GPI-AP having lost their fatty acid constituents (but retained the glycan core) during their release from cell surfaces into plasma. In fact, most GPI-AP have been identified as both membrane-anchored and soluble extracellular versions (39, 41). For instance, the GPI-AP, tissue nonspecific alkaline phosphatase, was found to be significantly elevated in the plasma of patients suffering from hypophosphatasia with mental retardation syndrome (4) as a consequence of defective GPI anchor remodeling, leading to release of tissue-nonspecific alkaline phosphatase from plasma membranes. Moreover, increased plasma concentrations of a soluble anchor-less version of the GPI-AP, urokinase plasminogen activator receptor, were measured for patients with paroxysmal nocturnal hemoglobinuria, which were in correlation with the number of mutant clonal cells and highest in patients developing thrombotic events in the following years (64). Chip-based sensing may enable single-step discrimination between GPI-AP harboring the complete GPI anchor, retaining a partial (lipolytically cleaved) anchor and having lost all anchor constituents due to proteolytic cleavage) in plasma, which would facilitate unraveling of structure-function relationships in disorders caused by defective GPI anchorage (36).

ACKNOWLEDGMENTS

We thank M. Bauer and P. Kotzbeck (Helmholtz Zentrum Munich, Institute for Diabetes and Obesity) for helpful discussions regarding EV. We also appreciate the collaborative help and experimental advice of Thomas Grönwold (SAW Inc.) for implementation of the SAW sensor technology.

GRANTS

This work is supported in part by funding to M. H. Tschöp from the Alexander von Humboldt Foundation, the Helmholtz Alliance ICAMED, and the Helmholtz Initiative on Personalized Medicine *iMed* by Helmholtz Association, and the Helmholtz cross-program topic "Metabolic Dysfunction" and the Initiative and Networking Fund of the Helmholtz Association.

DISCLOSURES

A. W. Herling is employed by a pharmaceutical company. He emphasizes that decisions of the company did not affect his contribution (design of experiments, analysis of data, interpretation of results, editing of the manuscript) to the study. No conflicts of interest, financial or otherwise, are declared by any other author. This declaration acknowledges that this paper adheres to the principles for transparent reporting and scientific rigor of preclinical research recommended by funding agencies, publishers, and other organizations engaged with supporting research.

AUTHOR CONTRIBUTIONS

G.A.M., A.W.H., K.S., and A.L. conceived and designed research; G.A.M. performed experiments; G.A.M. analyzed data; G.A.M., A.W.H., K.S., and A.L. interpreted results of experiments; G.A.M. prepared figures; G.A.M. drafted manuscript; G.A.M., A.L., and M.H.T. edited and revised manuscript; G.A.M., A.W.H., K.S., A.L., and M.H.T. approved final version of manuscript.

REFERENCES

- Anderson SM, Yu G, Giattina M, Miller JL. Intercellular transfer of a glycosylphosphatidylinositol (GPI)-linked protein: release and uptake of CD4-GPI from recombinant adeno-associated virus-transduced HeLa cells. *Proc Natl Acad Sci USA* 93: 5894–5898, 1996. doi:10.1073/pnas.93.12.5894.
- Andrä J, Böhlng A, Gronewold TMA, Schlecht U, Perpeet M, Gutsmann T. Surface acoustic wave biosensor as a tool to study the interaction of antimicrobial peptides with phospholipid and lipopoly-saccharide model membranes. *Langmuir* 24: 9148–9153, 2008. doi:10.1021/la801252t.
- Belachew D, Kazmerski T, Libman I, Goldstein AC, Stevens ST, Deward S, Vockley J, Sperling MA, Balest AL. Infantile hypophosphatasia secondary to a novel compound heterozygous mutation presenting with pyridoxine-responsive seizures. *JIMD Rep* 11: 17–24, 2013. doi:10.1007/8904_2013_217.
- Berman JD. Structural properties of acetylcholinesterase from eel electric tissue and bovine erythrocyte membranes. *Biochemistry* 12: 1710–1715, 1973. doi:10.1021/bi00733a008.
- Bobone S, Hilsch M, Storm J, Dunsing V, Herrmann A, Chiantia S. Phosphatidylserine lateral organization influences the interaction of influenza virus matrix protein 1 with lipid membranes. *J Virol* 91: e300267, 2017. doi:10.1128/JVI.00267-17.
- Bütikofer P, Kuypers FA, Xu CM, Chiu DT, Lubin B. Enrichment of two glycosyl-phosphatidylinositol-anchored proteins, acetylcholinesterase and decay accelerating factor, in vesicles released from human red blood cells. *Blood* 74: 1481–1485, 1989.
- Chatterjee P, Lim WL, Shui G, Gupta VB, James I, Fagan AM, Xiong C, Sohrabi HR, Taddei K, Brown BM, Benzinger T, Masters C, Snowden SG, Wenk MR, Bateman RJ, Morris JC, Martins RN. Plasma phospholipid and sphingolipid alterations in presenilin1 mutation carriers: A pilot study. *J Alzheimers Dis* 50: 887–894, 2016. doi:10.3233/JAD-150948.
- Ding X, Li P, Lin SC, Stratton ZS, Nama N, Guo F, Slotcavage D, Mao X, Shi J, Costanzo F, Huang TJ. Surface acoustic wave microfluidics. *Lab Chip* 13: 3626–3649, 2013. doi:10.1039/c3lc50361e.
- Dolezal S, Hester S, Kirby PS, Nairn A, Pierce M, Abbott KL. Elevated levels of glycosylphosphatidylinositol (GPI) anchored proteins in plasma from human cancers detected by C. septicum alpha toxin. *Cancer Biomark* 14: 55–62, 2014. doi:10.3233/CBM-130377.
- Eisenhaber B, Bork P, Eisenhaber F. Post-translational GPI lipid anchor modification of proteins in kingdoms of life: analysis of protein sequence data from complete genomes. *Protein Eng* 14: 17–25, 2001. doi:10.1093/protein/14.1.17.
- Ferguson MAJ, Haldar K, Cross GAM. Trypanosoma brucei variant surface glycoprotein has a sn-1,2-dimyristyl glycerol membrane anchor at its COOH terminus. *J Biol Chem* 260: 4963–4968, 1985.
- Ferreira GN, da-Silva AC, Tomé B. Acoustic wave biosensors: physical models and biological applications of quartz crystal microbalance. *Trends Biotechnol* 27: 689–697, 2009. doi:10.1016/j.tibtech.2009.09.003.
- Fogel R, Limson J, Seshia AA. Acoustic biosensors. *Essays Biochem* 60: 101–110, 2016. doi:10.1042/EBC20150011.
- Frick W, Bauer A, Bauer J, Wied S, Müller G. Structure-activity relationship of synthetic phosphoinositidylglycans mimicking metabolic insulin action. *Biochemistry* 37: 13421–13436, 1998. doi:10.1021/bi9806201.
- Gordon VM, Nelson KL, Buckley JT, Stevens VL, Tweten RK, Elwood PC, Leppla SH. Clostridium septicum alpha toxin uses glycosylphosphatidylinositol-anchored protein receptors. *J Biol Chem* 274: 27274–27280, 1999. doi:10.1074/jbc.274.38.27274.
- Gronewold TMA. Surface acoustic wave sensors in the bioanalytical field: recent trends and challenges. *Anal Chim Acta* 603: 119–128, 2007. doi:10.1016/j.aca.2007.09.056.
- Gronewold TMA, Glass S, Quandt E, Famulok M. Monitoring complex formation in the blood-coagulation cascade using aptamer-coated SAW sensors. *Biosens Bioelectron* 20: 2044–2052, 2005. doi:10.1016/j.bios.2004.09.007.
- Gronewold TMA, Schlecht U, Quandt E. Analysis of proteolytic degradation of a crude protein mixture using a surface acoustic wave sensor. *Biosens Bioelectron* 22: 2360–2365, 2007. doi:10.1016/j.bios.2006.09.013.
- Gruhl FJ, Rapp BE, Länge K. Biosensors for diagnostic applications. *Adv Biochem Eng Biotechnol* 133: 115–148, 2013. doi:10.1007/10_2011_130.
- Hattersley KJ, Hein LK, Fuller M. Lipid composition of membrane rafts, isolated with and without detergent, from the spleen of a mouse model of Gaucher disease. *Biochem Biophys Res Commun* 442: 62–67, 2013. doi:10.1016/j.bbrc.2013.11.009.
- Hazarosova R, Momchilova A, Koumanov K, Petkova D, Staneva G. Role of aminophospholipids in the formation of lipid rafts in model membranes. *J Fluoresc* 25: 1037–1043, 2015. doi:10.1007/s10895-015-1589-y.
- Hoener MC, Bolli R, Brodbeck U. Glycosyl-phosphatidylinositol-specific phospholipase D. Interaction with and stimulation by apolipoprotein A-I. *FEBS Lett* 327: 203–206, 1993. doi:10.1016/0014-5793(93)80170-Y.
- Hong Y, Ohishi K, Inoue N, Kang JY, Shime H, Horiguchi Y, van der Goot FG, Sugimoto N, Kinoshita T. Requirement of N-glycan on GPI-anchored proteins for efficient binding of aerolysin but not Clostrid-

- ium septicum alpha-toxin. *EMBO J* 21: 5047–5056, 2002. doi:10.1093/emboj/cdf508.
25. Howell S, Kenmore M, Kirkland M, Badley RA. High-density immobilization of an antibody fragment to a carboxymethylated dextran-linked biosensor surface. *J Mol Recognit* 11: 200–203, 1998. doi:10.1002/(SICI)1099-1352(199812)11:1/6<200:AID-JMR423>3.0.CO;2-7.
 26. Ilangumaran S, He H-T, Hoessli DC. Microdomains in lymphocyte signalling: beyond GPI-anchored proteins. *Immunol Today* 21: 2–7, 2000. doi:10.1016/S0167-5699(99)01494-2.
 27. Johnsson B, Löfås S, Lindquist G. Immobilization of proteins to a carboxymethyl-dextran-modified gold surface for biospecific interaction analysis in surface plasmon resonance sensors. *Anal Biochem* 198: 268–277, 1991. doi:10.1016/0003-2697(91)90424-R.
 28. Kausaitė-Minkstimiene A, Ramanaviciene A, Kirlyte J, Ramanavicius A. Comparative study of random and oriented antibody immobilization techniques on the binding capacity of immunosensor. *Anal Chem* 82: 6401–6408, 2010. doi:10.1021/ac100468k.
 29. Kooyman DL, Byrne GW, Logan JS. Glycosyl phosphatidylinositol anchor. *Exp Nephrol* 6: 148–151, 1998. doi:10.1159/000020516.
 30. Lahiri J, Isaacs L, Tien J, Whitesides GM. A strategy for the generation of surfaces presenting ligands for studies of binding based on an active ester as a common reactive intermediate: a surface plasmon resonance study. *Anal Chem* 71: 777–790, 1999. doi:10.1021/ac980959t.
 31. Landi APG, Wilson AB, Davies A, Lachmann PJ, Ferriani VP, Seilly DJ, Assis-Pandochi AI. Determination of CD59 protein in normal human serum by enzyme immunoassay, using octyl-glucoside detergent to release glycosyl-phosphatidylinositol-CD59 from lipid complex. *Immunol Lett* 90: 209–213, 2003. doi:10.1016/j.imlet.2003.07.001.
 32. Lee S, Kim YI, Kim KB. Comparative study of binding constants from Love wave surface acoustic wave and surface plasmon resonance biosensors using kinetic analysis. *J Nanosci Nanotechnol* 13: 7319–7324, 2013. doi:10.1166/jnn.2013.8082.
 33. Legler DF, Doucey M-A, Schneider P, Chapatte L, Bender FC, Bron C. Differential insertion of GPI-anchored GFPs into lipid rafts of live cells. *FASEB J* 19: 73–75, 2005. doi:10.1096/fj.03-1338fje.
 34. Lunkes GI, Lunkes DS, Morsch VM, Mazzanti CM, Morsch AL, Miron VR, Schetinger MR. NTPDase and 5'-nucleotidase activities in rats with alloxan-induced diabetes. *Diabetes Res Clin Pract* 65: 1–6, 2004. doi:10.1016/j.diabres.2003.11.016.
 35. Manček-Keber M, Frank-Bertoncelj M, Hafner-Bratkovič I, Smole A, Zorko M, Pirher N, Hayer S, Kralj-Iglič V, Rozman B, Ilc N, Horvat S, Jerala R. Toll-like receptor 4 senses oxidative stress mediated by the oxidation of phospholipids in extracellular vesicles. *Sci Signal* 8: ra60, 2015. doi:10.1126/scisignal.2005860.
 36. Manea E. A step closer in defining glycosylphosphatidylinositol anchored proteins role in health and glycosylation disorders. *Mol Genet Metab Rep* 16: 67–75, 2018. doi:10.1016/j.ymgmr.2018.07.006.
 37. Melzak KA, Bender F, Tsortos A, Gizeli E. Probing mechanical properties of liposomes using acoustic sensors. *Langmuir* 24: 9172–9180, 2008. doi:10.1021/la800730s.
 38. Müller JL. Release and extracellular transit of glycosylphosphatidylinositol proteins. *J Lab Clin Med* 131: 115–123, 1998. doi:10.1016/S0022-2143(98)90152-4.
 39. Müller GA. The release of glycosylphosphatidylinositol-anchored proteins from the cell surface. *Arch Biochem Biophys* 656: 1–18, 2018. doi:10.1016/j.abb.2018.08.009.
 40. Müller G. Microvesicles/exosomes as potential novel biomarkers of metabolic diseases. *Diabetes Metab Syndr* 5: 247–282, 2012. doi:10.2147/DMSO.S32923.
 41. Müller G, Bandlow W. Lipolytic membrane release of two phosphatidylinositol-anchored cAMP receptor proteins in yeast alters their ligand-binding parameters. *Arch Biochem Biophys* 308: 504–514, 1994. doi:10.1006/abbi.1994.1071.
 42. Müller G, Frick W. Signalling via caveolin: involvement in the cross-talk between phosphoinositolglycans and insulin. *Cell Mol Life Sci* 56: 945–970, 1999. doi:10.1007/s000180050485.
 43. Müller G, Hanekop N, Wied S, Frick W. Cholesterol depletion blocks redistribution of lipid raft components and insulin-mimetic signaling by glimepiride and phosphoinositolglycans in rat adipocytes. *Mol Med* 8: 120–136, 2002. doi:10.1007/BF03402005.
 44. Müller G, Jung C, Wied S, Welte S, Jordan H, Frick W. Redistribution of glycolipid raft domain components induces insulin-mimetic signaling in rat adipocytes. *Mol Cell Biol* 21: 4553–4567, 2001. doi:10.1128/MCB.21.14.4553-4567.2001.
 45. Müller G, Korndörfer A, Saar K, Karbe-Thönges B, Fasold H, Müllner S. 4'-Amino-benzamido-taurocholic acid selectively solubilizes glycosylphosphatidylinositol-anchored membrane proteins and improves lipolytic cleavage of their membrane anchors by specific phospholipases. *Arch Biochem Biophys* 309: 329–340, 1994. doi:10.1006/abbi.1994.1121.
 46. Müller G, Schneider M, Biemer-Daub G, Wied S. Microvesicles released from rat adipocytes and harboring glycosylphosphatidylinositol-anchored proteins transfer RNA stimulating lipid synthesis. *Cell Signal* 23: 1207–1223, 2011. doi:10.1016/j.cellsig.2011.03.013.
 47. Müller G, Schulz A, Wied S, Frick W. Regulation of lipid raft proteins by glimepiride- and insulin-induced glycosylphosphatidylinositol-specific phospholipase C in rat adipocytes. *Biochem Pharmacol* 69: 761–780, 2005. doi:10.1016/j.bcp.2004.11.014.
 48. Neumann S, Harterink M, Sprong H. Hitch-hiking between cells on lipoprotein particles. *Traffic* 8: 331–338, 2007. doi:10.1111/j.1600-0854.2006.00532.x.
 49. Nosjean O, Briolay A, Roux B. Mammalian GPI proteins: sorting, membrane residence and functions. *Biochim Biophys Acta* 1331: 153–186, 1997. doi:10.1016/S0304-4157(97)00005-1.
 50. Ogawa R, Tanaka C, Sato M, Nagasaki H, Sugimura K, Okumura K, Nakagawa Y, Aoki N. Adipocyte-derived microvesicles contain RNA that is transported into macrophages and might be secreted into blood circulation. *Biochem Biophys Res Commun* 398: 723–729, 2010. doi:10.1016/j.bbrc.2010.07.008.
 51. Onen O, Ahmad AA, Guldiken R, Gallant ND. Surface modification on acoustic wave biosensors for enhanced specificity. *Sensors (Basel)* 12: 12317–12328, 2012. doi:10.3390/s120912317.
 52. Oyarzún C, Salinas C, Gómez D, Jaramillo K, Pérez G, Alarcón S, Podestá L, Flores C, Quezada C, San Martín R. Increased levels of adenosine and ecto 5'-nucleotidase (CD73) activity precede renal alterations in experimental diabetic rats. *Biochem Biophys Res Commun* 468: 354–359, 2015. doi:10.1016/j.bbrc.2015.10.095.
 53. Raghupathy R, Anilkumar AA, Polley A, Singh PP, Yadav M, Johnson C, Suryawanshi S, Saikam V, Sawant SD, Panda A, Guo Z, Vishwakarma RA, Rao M, Mayor S. Transbilayer lipid interactions mediate nanoclustering of lipid-anchored proteins. *Cell* 161: 581–594, 2015. doi:10.1016/j.cell.2015.03.048.
 54. Rifkin MR, Landsberger FR. Trypanosome variant surface glycoprotein transfer to target membranes: a model for the pathogenesis of trypanosomiasis. *Proc Natl Acad Sci USA* 87: 801–805, 1990. doi:10.1073/pnas.87.2.801.
 55. Rooney IA, Davies A, Morgan BP. Membrane attack complex (MAC)-mediated damage to spermatozoa: protection of the cells by the presence on their membranes of MAC inhibitory proteins. *Immunology* 75: 499–506, 1992.
 56. Rooney IA, Heuser JE, Atkinson JP. GPI-anchored complement regulatory proteins in seminal plasma. An analysis of their physical condition and the mechanisms of their binding to exogenous cells. *J Clin Invest* 97: 1675–1686, 1996. doi:10.1172/JCI118594.
 57. Saha S, Anilkumar AA, Mayor S. GPI-anchored protein organization and dynamics at the cell surface. *J Lipid Res* 57: 159–175, 2016. doi:10.1194/jlr.R062885.
 58. Saitakis M, Gizeli E. Acoustic sensors as a biophysical tool for probing cell attachment and cell/surface interactions. *Cell Mol Life Sci* 69: 357–371, 2012. doi:10.1007/s00018-011-0854-8.
 59. Sargiacomo M, Sudol M, Tang Z, Lisanti MP. Signal transducing molecules and glycosyl-phosphatidylinositol-linked proteins form a caveolin-rich insoluble complex in MDCK cells. *J Cell Biol* 122: 789–807, 1993. doi:10.1083/jcb.122.4.789.
 60. Seong J, Wang Y, Kinoshita T, Maeda Y. Implications of lipid moiety in oligomerization and immunoreactivities of GPI-anchored proteins. *J Lipid Res* 54: 1077–1091, 2013. doi:10.1194/jlr.M034421.
 61. Shlomovitz R, Schick M. Model of a raft in both leaves of an asymmetric lipid bilayer. *Biophys J* 105: 1406–1413, 2013. doi:10.1016/j.bpj.2013.06.053.
 62. Simons K, Toomre D. Lipid rafts and signal transduction. *Nat Rev Mol Cell Biol* 1: 31–39, 2000. doi:10.1038/35036052.
 63. Sloand EM, Maciejewski JP, Dunn D, Moss J, Brewer B, Kirby M, Young NS. Correction of the PNH defect by GPI-anchored protein transfer. *Blood* 92: 4439–4445, 1998.
 64. Sloand EM, Pfannes L, Scheinberg P, More K, Wu CO, Horne M, Young NS. Increased soluble urokinase plasminogen activator receptor (suPAR) is associated with thrombosis and inhibition of plasmin genera-

- tion in paroxysmal nocturnal hemoglobinuria (PNH) patients. *Exp Hematol* 36: 1616–1624, 2008. doi:10.1016/j.exphem.2008.06.016.
65. Stadelmann B, Büttikofer P, König A, Brodbeck U. The C-terminus of glycosylphosphatidylinositol-specific phospholipase D is essential for biological activity. *Biochim Biophys Acta* 1355: 107–113, 1997. doi:10.1016/S0167-4889(96)00119-X.
 66. Stemmer K, Bieloheby M, Grayson BE, Begg DP, Chambers AP, Neff C, Woods SC, Erben RG, Tschöp MH, Bidlingmaier M, Clemens TL, Seeley RJ. Roux-en-Y gastric bypass surgery but not vertical sleeve gastrectomy decreases bone mass in male rats. *Endocrinology* 154: 2015–2024, 2013. doi:10.1210/en.2012-2130.
 67. Suzuki KGN, Kasai RS, Hirosawa KM, Nemoto YL, Ishibashi M, Miwa Y, Fujiwara TK, Kusumi A. Transient GPI-anchored protein homodimers are units for raft organization and function. *Nat Chem Biol* 8: 774–783, 2012. doi:10.1038/nchembio.1028.
 68. Taguchi R, Ikezawa H. Properties of bovine erythrocyte acetylcholinesterase solubilized by phosphatidylinositol-specific phospholipase C1. *J Biochem* 102: 803–811, 1987. doi:10.1093/oxfordjournals.jbchem.a122119.
 69. Taguchi R, Suzuki K, Nakabayashi T, Ikezawa H. Acetylcholinesterase release from mammalian erythrocytes by phosphatidylinositol-specific phospholipase C of *Bacillus thuringiensis* and characterization of the released enzyme. *J Biochem* 96: 437–446, 1984. doi:10.1093/oxfordjournals.jbchem.a134855.
 70. Väkevää A, Jauhiainen M, Ehnholm C, Lehto T, Meri S. High-density lipoproteins can act as carriers of glycoposphoinositol lipid-anchored CD59 in human plasma. *Immunology* 82: 28–33, 1994.
 71. van Meer G, Voelker DR, Feigenson GW. Membrane lipids: where they are and how they behave. *Nat Rev Mol Cell Biol* 9: 112–124, 2008. doi:10.1038/nrm2330.
 72. Voiculescu I, Nordin AN. Acoustic wave based MEMS devices for biosensing applications. *Biosens Bioelectron* 33: 1–9, 2012. doi:10.1016/j.bios.2011.12.041.
 73. von Toerne C, Huth C, de Las Heras Gala T, Kronenberg F, Herder C, Koenig W, Meisinger C, Rathmann W, Waldenberger M, Roden M, Peters A, Thorand B, Hauck SM. MASP1, THBS1, GPLD1 and ApoA-IV are novel biomarkers associated with prediabetes: the KORA F4 study. *Diabetologia* 59: 1882–1892, 2016. doi:10.1007/s00125-016-4024-2.
 74. Wei H, Malcor JM, Harper MT. Lipid rafts are essential for release of phosphatidylserine-exposing extracellular vesicles from platelets. *Sci Rep* 8: 9987, 2018. doi:10.1038/s41598-018-28363-4.
 75. Wurtman R. Biomarkers in the diagnosis and management of Alzheimer's disease. *Metabolism* 64, Suppl 1: S47–S50, 2015. doi:10.1016/j.metabol.2014.10.034.
 76. Yáñez-Mó M, Siljander PR, Andreu Z, Zavec AB, Borràs FE, Buzas EI, Buzas K, Casal E, Cappello F, Carvalho J, Colás E, Cordeiro-da Silva A, Fais S, Falcon-Perez JM, Ghobrial IM, Giebel B, Gimona M, Graner M, Gursel I, Gursel M, Heegaard NH, Hendrix A, Kierulf P, Kokubun K, Kosanovic M, Kralj-Iglic V, Krämer-Albers EM, Laitinen S, Lässer C, Lener T, Ligeti E, Linē A, Lipps G, Llorente A, Lötvall J, Manček-Keber M, Marcilla A, Mittelbrunn M, Nazarenko I, Nolte-t Hoen EN, Nyman TA, O'Driscoll L, Olivan M, Oliveira C, Pállinger É, Del Portillo HA, Reventós J, Rigau M, Rohde E, Sammar M, Sánchez-Madrid F, Santarém N, Schallmoser K, Ostenfeld MS, Stoorvogel W, Stukelj R, Van der Grein SG, Vasconcelos MH, Wauben MH, De Wever O. Biological properties of extracellular vesicles and their physiological functions. *J Extracell Vesicles* 4: 27066, 2015. doi:10.3402/jev.v4.27066.
 77. Zhang B, Yang Y, Xiang L, Zhao Z, Ye R. Adipose-derived exosomes: a novel adipokine in obesity-associated diabetes. *J Cell Physiol*. In press. doi:10.1002/jcp.28354.
 78. Zhou J, Li YS, Chien S. Shear stress-initiated signaling and its regulation of endothelial function. *Arterioscler Thromb Vasc Biol* 34: 2191–2198, 2014. doi:10.1161/ATVBAHA.114.303422.

